

DYNAMIC RESPONSE CHARACTERISTICS OF THE FATIH MOSQUE IN
ISTANBUL ESTIMATED FROM EARTHQUAKE DATA

by

Ayşe Tongut

B.S., Civil Engineering, Dokuz Eylül University, 2015

Submitted to the Kandilli Observatory and Earthquake
Research Institute in partial fulfillment of
the requirements for the degree of
Master of Science

Graduate Program in Earthquake Engineering
Boğaziçi University

2017

ACKNOWLEDGEMENTS

I would first like to express my deepest appreciation to my advisor Prof. Eser aktı for her full support, expert guidance, understanding and encouragement throughout my study and research. In addition, I express my appreciation to Prof. Erdal Şafak, the door to Prof. Şafak office was always open whenever I ran into a trouble spot or had a question about my research.

I would also like to thank Ahmet Korkmaz for working devotedly on the collection of data. I am so glad to work with helpful and gracious friends. I wish to express my great thanks to Mahir, Tlay for their patience and guidance on my thesis. I also want to express my special thanks to my friend Berkay Bykarda for his supports and advices.

Finally, I would like to thank my mother, father and brother for their unconditional love and support during this study and in all my experience.

ABSTRACT

DYNAMIC RESPONSE CHARACTERISTICS OF THE FATIH MOSQUE IN ISTANBUL ESTIMATED FROM EARTHQUAKE DATA

Structural Health Monitoring (SHM) enables continuous recording of the dynamic response of a structure and analysis of its time-varying dynamic characteristics for condition and ultimately damage assessment. SHM is increasingly used for the estimation of dynamic behavioral characteristics of historical structures, which is vital for conservation, repair and strengthening. For the preservation of the architectural heritage, a crucial element in our present-day culture, the historical constructions need to be identified both in terms of their structural system and present damages. The Fatih Mosque in Istanbul is part of a larger complex. The first mosque was built soon after the conquest of Constantinople between the years 1463 and 1470. After 1766 earthquake the first mosque collapsed. The present mosque built in 1771 and is one of the most significant monuments in the city. In this study, the four-year monitoring data (2013-2016) recorded by the Fatih Mosque Structural Health Monitoring System is analyzed. The vibration monitoring system in the Fatih Mosque consists of thirteen three-component accelerometers and four two-component tilt-meters. During the four year period, the mosque experienced more than 160 earthquakes whose magnitudes varied between 2.1 and 6.5 in the Richter scale. A database of recordings suitable for further analysis is created by applying selection criteria for number of recording stations, signal to noise ratio, epicentral distance and earthquake magnitude. The data is uniformly processed using computer codes developed in MATLAB. Time domain and frequency domain characteristics of structural response are studied with the help of recorded earthquakes in the structure. Additionally presence of soil-structure interaction and rocking; and variations in wave travel times are investigated.

ÖZET

İSTANBUL FATİH CAMİİ'NİN DİNAMİK ÖZELLİKLERİNİN DEPREM VERİLERİ İLE BELİRLENMESİ

Yapı sağlığı izleme, yapıların zamana bağlı değişen dinamik özelliklerini tanımlamak ve mevcut hasarları tespit etmek amacı ile yapıların kesintisiz olarak izlendiği bir sistemdir. Yapı sağlığı izleme tarihi yapıların korunması, onarılması ve güçlendirilmesi için gerekli çalışmalarda kullanılacak olan modal özelliklerini belirlemek için kullanılan yaygın bir metottür. Tarihi yapıların korunması modern hayatın kültürel yaşamında oldukça önemlidir. Bu kültürel mirasların korunması için, tarihi yapıların yapı sistemi özellikleri ve mevcut hasarlarının belirlenmesi önemlidir. Fatih Camii ve Külliyesi 1463 ile 1470 yılları arasında Fatih şehri fethettikten kısa bir süre sonra inşa edilmiş olup İstanbul'daki en önemli eserlerden biridir. Bu çalışmada, Fatih Camisinde kaydedilmiş dört yıllık deprem verisi işlenmiştir. Fatih Camii izleme sistemi 13 adet ivmeölçer ve 4 adet tilt-metreden oluşmaktadır. Her ivmeölçer 3 kanallı olup 2013 yılında 100 Hz, 2013'ten sonra ise 200 Hz ile değiştirilmiş olup bugün de halen aynı frekansta faaliyet göstermektedir. Dört yıllık dönem boyunca, camii Richter ölçüsünde büyüklükleri 2,1 ile 6,5 arasında değişen 160'dan fazla deprem deneyimlemiştir. Fakat bu deprem verisine bazı kısıtlamalar uygulanmış (düşük sinyal-gürültü oranı, bütün cihazla tarafından kayıtlanamamış, mesafe ve büyüklük değerleri vs.) ve böylece hepsi analizlerde kullanılmamıştır. Bununla beraber, veri tabanı büyüklük, mesafe ve azimuta bağlı fonksiyonlar olarak gruplandırılmıştır. Elde edilmiş veri tabanı frekans alanı ve mod şekilleri tekniklerini Matlab'de geliştirilen kodlar kullanılarak analiz edilmiştir. Zemin-yapı etkileşimi ve rijit yapı titreşimlerinin yapının dinamik davranışına etkisi incelenmiştir. Son olarak, yapıdaki mevcut hasarlar dalga ulaşım hızı ve zamanı araştırarak incelenmiştir.

TABLE OF CONTENTS

ACKNOWLEDGEMENTS	iii
ABSTRACT	iv
ÖZET	v
LIST OF FIGURES	viii
LIST OF TABLES	xiv
LIST OF ACRONYMS/ABBREVIATIONS	xv
1. INTRODUCTION	1
1.1. Objective	1
1.2. Organization	1
1.3. Structural Health Monitoring	2
1.4. Modal Analysis	2
1.5. Frequency Change	3
1.6. Soil-Structure Interaction	4
1.7. Wave Travel Time	4
2. FATİH MOSQUE	6
2.1. The History of the Fatih Mosque	6
2.2. Damage and Repair History	7
2.3. Architectural History	9
2.3.1. The Old Mosque	9
2.3.2. The New Mosque	10
2.4. The Restoration of Fatih Mosque Between 2007-2012	11
2.4.1. Restoration	11
2.4.2. Strengthening	12
3. METHODOLOGY	15
3.1. Fatih Mosque Structural Health Monitoring System	15
3.2. Earthquake Data	18
3.3. Data Processing	24
3.3.1. Filtering	25
3.3.2. Smoothing	25

4. EARTHQUAKE RESPONSE	29
4.1. TIME DOMAIN CHARACTERISTICS	29
4.2. Frequency Domain Characteristics	40
4.2.1. Modal Frequencies	40
4.2.2. Mode Shapes	44
4.2.3. Frequency Change	52
5. SOIL-STRUCTURE INTERACTION	54
5.1. Soil-Structure Interaction	54
5.2. Soil Effect	62
6. ROCKING	68
7. WAVE TRAVELS	73
8. CONCLUSION	74
REFERENCES	75

LIST OF FIGURES

Figure 2.1.	Old Mosque’s Plan (Ayverdi, 1973)	9
Figure 2.2.	New Mosque’s Plan (Gurlitt)	10
Figure 2.3.	General View of the Mosque.	11
Figure 2.4.	Separations in the minaret’s stone	13
Figure 2.5.	Application of stainless steel clamp	13
Figure 2.6.	The old peripheral tie beam	13
Figure 2.7.	The disfunctional timber tie beams	14
Figure 3.1.	Fatih Mosque Structural Health Monitoring System, plan view (Gurlitt)	16
Figure 3.2.	Instrument layout in section, X-axis	17
Figure 3.3.	Instrument layout in section, Y-axis	17
Figure 3.4.	Fatih Mosque SHM system, interior view (TripAdvisor)	18
Figure 3.5.	General Location of Fatih Mosque (Google Earth).	19
Figure 3.6.	Epicenters of Earthquakes (1) (Google Earth).	20
Figure 3.7.	Epicenters of Earthquakes (2) (Google Earth).	20

Figure 3.8.	Magnitude Histogram.	21
Figure 3.9.	Distance Histogram.	22
Figure 3.10.	Azimuthal Map.	23
Figure 3.11.	Azimuthal Histogram.	23
Figure 3.12.	Azimuthal Location of Fatih Mosque (Google Earth)	24
Figure 4.1.	Acceleration time history of 6.5 Aegean Sea earthquake	30
Figure 4.2.	Velocity time history of 6.5 Aegean Sea earthquake	31
Figure 4.3.	Displacement time history of 6.5 Aegean Sea earthquake	32
Figure 4.4.	Acceleration time history of 4.4 Yalova earthquake	33
Figure 4.5.	Velocity time history of 4.4 Yalova earthquake	34
Figure 4.6.	Displacement time history of 4.4 Yalova earthquake	35
Figure 4.7.	Peak Horizontal accelerations in X direction recorded at Fatih Mosque	36
Figure 4.8.	Peak Horizontal accelerations in Y direction recorded at Fatih Mosque	36
Figure 4.9.	Peak Horizontal velocities in X direction recorded at Fatih Mosque	37
Figure 4.10.	Peak Horizontal velocities in Y direction recorded at Fatih Mosque	37

Figure 4.11. Peak Horizontal displacements in X direction recorded at Fatih Mosque	38
Figure 4.12. Peak Horizontal displacements in Y direction recorded at Fatih Mosque	38
Figure 4.13. Peak Ground Acceleration vs Magnitude	39
Figure 4.14. Peak Ground Velocity vs Magnitude	39
Figure 4.15. Peak Ground Displacement vs Magnitude	40
Figure 4.16. Horizontal (X) top-to-basement Transfer Function of 6.5 Aegean Sea earthquake	42
Figure 4.17. Horizontal (Y) top-to-basement Transfer Function of 6.5 Aegean Sea earthquake	42
Figure 4.18. Horizontal (X) top-to-basement Transfer Function of 5.0 Black Sea earthquake	43
Figure 4.19. Horizontal (Y) top-to-basement Transfer Function of 5.0 Black Sea earthquake	43
Figure 4.20. Particle motion of the mosque during 6.5 Aegean Sea earthquake .	46
Figure 4.21. Response of the mosque to 5.6 Romania earthquake (Filtered between 2.3 Hz to 2.5 Hz)	47
Figure 4.22. Response of the mosque to 6.5 Aegean Sea earthquake (Filtered between 2.55 Hz to 2.80 Hz)	48

Figure 4.23. Response of the mosque to 4.4 Yalova earthquake (Filtered between 3.21 Hz to 3.60 Hz)	49
Figure 4.24. Response of the mosque to 4.0 Yalova earthquake (Filtered between 5.7 Hz to 6.1 Hz)	50
Figure 4.25. Response of the mosque to 4.0 Yalova earthquake (Filtered between 7.7 Hz to 8.2 Hz)	51
Figure 4.26. Frequency drop in X direction in percent, horizontal axis is the peak ground acceleration at station ZEM, vertical axis is the frequency change at station KUB3	52
Figure 4.27. Frequency drop in Y direction in percent, horizontal axis is the peak ground acceleration at station ZEM, vertical axis is the frequency change at station KUB3	53
Figure 5.1. Earthquakes used in analysis	54
Figure 5.2. Horizontal (X) Fourier Amplitude Spectra of 6.5 Aegean Sea earthquake	55
Figure 5.3. Horizontal (X) top-to-basement Transfer Function of 6.5 Aegean Sea earthquake	55
Figure 5.4. Horizontal (Y) Fourier Amplitude Spectra of 6.5 Aegean Sea earthquake	56
Figure 5.5. Horizontal (Y) top-to-basement Transfer Function of 6.5 Aegean Sea earthquake	56

Figure 5.6.	Horizontal (X) Fourier Amplitude Spectra of 4.0 Yalova earthquake	57
Figure 5.7.	Horizontal (X) top-to-basement Transfer Function of 4.0 Yalova earthquake	57
Figure 5.8.	Horizontal (Y) Fourier Amplitude Spectra of 4.0 Yalova earthquake	58
Figure 5.9.	Horizontal (Y) top-to-basement Transfer Function of 4.0 Yalova earthquake	58
Figure 5.10.	Horizontal (X) Fourier Amplitude Spectra of 5.0 Black Sea earthquake	59
Figure 5.11.	Horizontal (X) top-to-basement Transfer Function of 5.0 Black Sea earthquake	59
Figure 5.12.	Horizontal (Y) Fourier Amplitude Spectra of 5.0 Black Sea earthquake	60
Figure 5.13.	Horizontal (Y) top-to-basement Transfer Function of 5.0 Black Sea earthquake	60
Figure 5.14.	Horizontal (X) Fourier amplitude spectra of earthquakes recorded in ZEM station	63
Figure 5.15.	Horizontal (Y) Fourier amplitude spectra of earthquakes recorded in ZEM station	63
Figure 5.16.	Vertical (Z) Fourier amplitude spectra of earthquakes recorded in ZEM station	64
Figure 5.17.	Horizontal (X) Fourier amplitude spectra of earthquakes recorded in down-hole	64

Figure 5.18.	Horizontal (Y) Fourier amplitude spectra of earthquakes recorded in down-hole	65
Figure 5.19.	Vertical (Z) Fourier amplitude spectra of earthquakes recorded in down-hole	65
Figure 5.20.	Horizontal to vertical spectral ratio of Fas of down-hole surface array of Fatih	66
Figure 5.21.	Horizontal to vertical spectral ratio of Fas of ZEM station of Fatih	67
Figure 6.1.	Fourier amplitude spectrum of vertical ZEM and horizontal components (X and Y) of GAL1, GAL2, GAL3, GAL4 stations	69
Figure 6.2.	FAS of 6.5 Aegean Sea Earthquake (X direction)	71
Figure 6.3.	TF of 6.5 Aegean Sea Earthquake (X direction)	71
Figure 6.4.	FAS of 6.5 Aegean Sea Earthquake (Y direction)	72
Figure 6.5.	TF of 6.5 Aegean Sea Earthquake (Y direction)	72

LIST OF TABLES

Table 3.1.	Earthquakes recorded between 2013 (Jan) and 2014 (June) in Fatih Mosque	26
Table 3.2.	Earthquakes recorded between 2014 (Dec) and 2015 (May) in Fatih Mosque	27
Table 3.3.	Earthquakes recorded between 2015 (May) and 2017 (Feb) in Fatih Mosque	28
Table 4.1.	Modal Frequencies	41
Table 4.2.	Applied band-pass filter around modal frequencies	45
Table 5.1.	Fundamental frequencies apparent on horizontal (Y) FAS and TF	61
Table 5.2.	Fundamental frequencies apparent on horizontal (X) FAS and TF	61

LIST OF ACRONYMS/ABBREVIATIONS

2D	Two Dimensional
3D	Three Dimensional
SHM	Structural Health Monitoring
SSI	Soil-Structure Interaction

1. INTRODUCTION

1.1. Objective

The main purpose of this study is to identify the dynamic response characteristics of the Fatih Mosque in Istanbul. Time domain and frequency domain characteristics of structural response are studied with the help of recorded earthquakes in the structure. Additionally presence of soil-structure interaction and rocking; and variations in wave travel times are investigated.

Fatih Mosque, also known as the Conqueror's mosque in English, is located in a district of the Old City of Istanbul named after the mosque. The mosque has a long history of earthquake damages. It was last damaged by the 1999 Kocaeli Earthquake and restored between the years 2007 and 2012.

One of the most powerful excitation sources for structures is the earthquake ground motion. Structures which are instrumented with strong motion accelerometers benefit from recorded seismic events, as their analysis provide direct evidence of structural earthquake response. In this study strong ground motions recorded by the Fatih Mosque Structural Health Monitoring System during earthquakes over a four-year time period are analyzed.

1.2. Organization

Organization of thesis is such that, following the introduction, first description of the mosque including its historical and architectural features and damage history are presented followed by a summary of the most recent restoration and strengthening works. Next, an overview of the strong motion monitoring system of the mosque and of the earthquakes experienced by the mosque and recorded by the system since its first installation are given. Afterwards, assessments of modal frequencies and mode shapes, time domain behavioral characteristics, investigations on the presence of soil structure

interaction and rocking; and possible variations in wave travel times are presented. In the last chapter, conclusions of the study are summarized.

1.3. Structural Health Monitoring

Structural Health Monitoring (SHM) is a system for continuous monitoring of structures to identify their dynamic characteristics as well as to detect changes in their dynamic properties due to factors such as earthquakes, winds and other environmental factors. Using data from SHM systems it is also possible to detect anomalies that potentially could be associated with damage. SHM systems consist of sensors such as accelerometers, displacement meters, GPS sensors and tiltmeters; and of elements for data communication, analysis and recording. The layout, type and location of sensors are essential for a useful observation. The layout and location of sensors generally depend on the geometry and structural behavior characteristics of the building to be monitored. The sensors are generally positioned at locations to deduce optimum data and thus information on structural response and ultimately damage.

Parallel to the developments in computer science; communication, sensor and recording technologies, there has been a rapid increase in the number of structures with SHM systems. SHM systems have been installed in different kinds of structures especially in tall buildings, bridges and historical structures. The data obtained from these monitoring systems have been useful in understanding the nature of dynamic behavior of these structures. However, there has been no published standard for data analysis and data interpretation.

1.4. Modal Analysis

On the basis of evidence currently available, it seems fair to suggest that for improvement and development of earthquake design codes it is essential to understand the nature of the dynamic response of the structures which requires identification of the natural frequencies of vibration, mode shapes and corresponding equivalent damping.

In structural engineering, modal analysis is a standard approach to analyze the earthquake response of structures. The main theoretical premise behind identifying dynamic properties of structures is Fourier type analysis that provides the natural frequencies, damping and modal shapes of systems. Fourier analysis is the most common way to estimate modal properties.

To gain knowledge on dynamic properties, structural response to forced vibrations (i.e. requires full scale testing) and response to small amplitude excitations due to ambient vibrations or low-magnitude earthquakes, should be analyzed properly. Once identified, these properties can be used in modeling and assessments of linear structural response. Analysis of data from sources of excitation resulting in higher amplitude vibrations, such as medium-to-large magnitude earthquakes are used in the estimation of structural response in the non-linear range.

In this sense, it will be seen that complete measurements covering a wide amplitude and frequency range have been rather useful for understanding the dynamic response of the Fatih Mosque studied in this thesis.

1.5. Frequency Change

It is known that dominant frequencies of vibration are dependent on the properties of underlying soils, foundation and superstructure. Moreover they tend to vary as a function of vibration amplitude, duration of shaking and environmental factors. Udvardia and Trifunac demonstrated that during ground shaking, the apparent frequencies can reduce substantially, yet may return moderately or absolutely [1]. Todorovska *et al.* claimed that to estimate period lengthening is crucial to develop the building codes and studied the variations of the system frequencies of 21 buildings in the Los Angeles area which recorded three strong earthquakes (Northridge (MS= 6.7), San Fernando (ML = 6.6) and the 1987 Whittier Narrows (ML = 5.9)), and their aftershocks [2]. For their data set, the drop in frequencies did not exceed 30%. Furthermore, the current literature on frequency change abounds with examples of temporary changes due to environmental factors such as temperature, wind and rainfall [3] .

1.6. Soil-Structure Interaction

The presence of SSI can cause a significant change in the frequency content of seismic response of a structure. In reality all buildings are subjected to SSI, but when it is small the effect of upper stories' motion on the foundation level is negligible. In such a case the building can be assumed as fixed-based and recordings from foundation level can be considered as base excitation. However, if the building is subjected to SSI upper stories' motion can influence the foundation level motions, and records from the foundation cannot be taken as base excitation. Such a system is considered as a closed-loop dynamic system, meaning the input and the output are coupled [4]. In such cases, SSI effect should be taken into account in numerical models.

No systematic attempt has been made to identify the SSI in historical structures. Yet, Safak showed a process for the identification of SSI effects in buildings when there are no down-hole or free-field motions available [5]. It is relatively easy to identify the SSI effect if down-hole or free-field records and records of foundations of buildings are available. The common conclusion is that the fundamental frequencies in the presence of SSI are always below the frequencies with the case of no SSI, i.e. the fixed-based buildings. In this study, the procedure is followed to investigate the presence of SSI in the case of the Fatih Mosque. The earthquakes recorded by the nearby down-hole array located within the complex are analyzed for investigation of the effects of SSI, and the results are compared with those obtained using data from the foundation recorder in the mosque [5].

1.7. Wave Travel Time

Earthquakes produce transmitted seismic waves which travel in all directions through the Earth's layers. Seismic waves are not able to propagate in the air, so they are reflected back from the free surface into the earth. But if a structure exists on the surface, the waves move into the structure causing structural vibrations. In other words, during earthquakes seismic waves propagate into the structure and cause the structure to vibrate.

Even though seismic waves propagate into the structure and cause the structure to vibrate, the wave propagation approach is not widely used for analyzing seismic response of structures. Traditionally the structures are modeled as a continuum medium. Uzdiger and Aydogan [6] used wave propagation approach to calculate un-damped response of masonry structures. Safak showed a discrete-time formulation of the seismic response of tall buildings using wave propagation approach [5].

Examining the changes in measured vibration response is a method to detect, locate and characterize anomalies and ultimately damage in structural systems. The basic idea behind this method is that modal parameters like modal frequencies and mode shapes are functions of physical properties of the structure such as stiffness and mass, meaning changes in physical properties cause changes in modal properties. Even at small amplitude excitation levels structures might exhibit non-linear response, yet it cannot be detectable from the changes in system natural frequencies. Another way to investigate local and global damages is to calculate wave travel times in the structure. Because modal analysis does not provide the local features, wave-propagation formulation provides an alternative for identification and localization of damage and its future detection.

2. FATI H MOSQUE

2.1. The History of the Fatih Mosque

Constantinople was one of the prominent centers of the western world until Mehmet II (1451-1481) conquered the city. After he took Constantinople in 1453, Istanbul was declared as the new capital of the Ottoman Empire replacing Edirne. At the time of the conquest Byzantine Empire was deprived, reduced in size and in need of financial help. Mehmed II wanted to revitalize Istanbul, to organize it as his central seat to govern and develop the Ottoman domain. In line with this target, Mehmed II repopulated the new capital by bringing in a great number of Greeks, Armenian and Turks. The population of the new capital was only 30000. He converted Hagia Sophia into a mosque. He continued his campaigns into the Balkans and visited Acropolis in Athens in 1456. He spent four days in Athens studying the Greek legacy. Upon his return to the capital, as part of his comprehensive strategy he decided to establish an academy, which is envisioned as a center of famous scholars educating administrative and military personnel [7] .

Mehmed II had his mosque, the Fatih Mosque, and its complex designed and built by the Architect Atik Sinan (b.? - d. Istanbul, 1471). The construction lasted for about eight years between 1463 and 1470. The mosque is located on the fourth hill of Istanbul, in today's Fatih district, it almost occupies the same site of the Church of Holy Apostles built by Justinian I (527-565). The Church of Holy Apostles was already collapsed and its materials were used for the construction of Fatih's complex [7] .

The complex (külliye), includes eight madrasahs (medrese), a hospice (tabhane), a big public kitchen (imaret), a hospital (darüŝ-ŝifa), a caravanserai, and rooms for student accommodation, and a refectory [8]. The tombs of Mehmed II and his wife and the mother of Beyazit II, Gülbahar Hatun, are also within the complex [7].

2.2. Damage and Repair History

Fatih mosque, built by Architect Atik Sinan by the order of Sultan Mehmed II, between 1463 and 1470, was first damaged during the 1509 earthquake and subsequently repaired. The structure survived many earthquakes between 1509 and 1766 with varying damages. In the 1766 earthquake the building was heavily damaged and its central dome collapsed. The mosque was reconstructed in 1771 by Architect Mehmet Tahir, during the reign of Mustafa III [9]. It is shown by various researchers that the old mosque had an architectural configuration other than the current one [10]. Today, the mosque's crown gate, mihrab and lower parts of its minarets are the parts that survived the original elements. Moreover, three wings of ablution fountain's (sadirvan) courtyard are among the parts that survived to this day [9].

Historically the hill on which the Fatih mosque is located, has been a site of prominent structures. However, most of these structures received some sort of structural damage reaching heavy damage and total collapse due to earthquakes. A chronological list that shows historical structures built on the site and damages due to a series of hazards is given below after [8–10]:

Our interest that is Fatih Mosque has also experienced frequent earthquakes and received various level of damages since it built. A chronological list that shows historical structures and damage done by earthquakes is given below:

(i) East Roman Period

- 330-337 AD – Construction of Holy Apostles Church
- 358 Earthquake – Collapse after severe damage
- 550 AD- Reconstruction of Holy Apostles Church
- 1010 Earthquake – Dome collapse
- 1296 Earthquake – Total collapse

(ii) Ottoman Period

- 1462-1470 – Construction of Fatih Mosque (By Atik Sinan)
- 1509 Earthquake –The capitals of four great columns cracked and the main

dome was badly cleft. Minarets were thrown down. Sultan's loge collapsed. Sultan Beyazıd the second made the Sultan's loge built as wooden.

- 1556 Earthquake - Damaged and restored.
- 1633 The great İstanbul fire – Spires burned.
- 1648 Earthquake -Damaged and restored.
- 1698 – Dome was damaged as the result of Gunpowder factory explosion in Şehremini.
- 1754 Earthquake - Damaged and restored.
- 1766 Earthquake – Total collapse. The original form of the mosque was destroyed in the 1766 earthquake.
- 1772 – Sultan Mustafa II undertook its reconstruction and the present building was completed.
- 1782 The Great Fire – Fatih Mosque and its complex damaged severely and restored.
- 1858- 1860 – Overall repair.
- 1879 – One of the spires of a minaret collapsed and the other damaged seriously because of wind. Minarets rebuilt with stone materials.
- 1880 – Spires collapsed due to wind.
- 1886 – Minarets repaired.
- 1894 Earthquake – Minarets damaged badly.
- 1907 - Overall repair.

(iii) Republic Era

- 1999 Izmit Earthquake – Fatih Mosque and Mahmut I. Library which is adjacent to the southern wall of the mosque were last affected by the earthquake and cracks have occurred in the whole structure.
- 2007-2012 – Fatih Mosque Restoration and Strengthening Applications

As a conclusion, as one of the İstanbul's oldest and most important religious structures, this monument has been repaired and renovated many times because of earthquakes, fires, tornados, storms and decay. As a result most of its parts has been changed and rebuilt.

2.3. Architectural History

2.3.1. The Old Mosque

The earthquakes badly damaged the original mosque designed by Atik Sinan in 1509. It was subsequently repaired, but the 1557 and 1754 earthquakes damaged the mosque again. Although the mosque was repaired immediately and kept standing, it could not resist the 1766 earthquake. There have been some proposals about the original plan of the mosque based on the print by Melchior Lorich (1559) and also on *Seyahatname* by Evliya Celebi (17th century). In light of sketches and descriptions of travelers and chroniclers, it is believed that the old mosque had a plan with a 26 meter diameter main dome in the center, a single semi-dome on the mihrab side and three small domes to extend the mosque in plan (Figure 2.1).

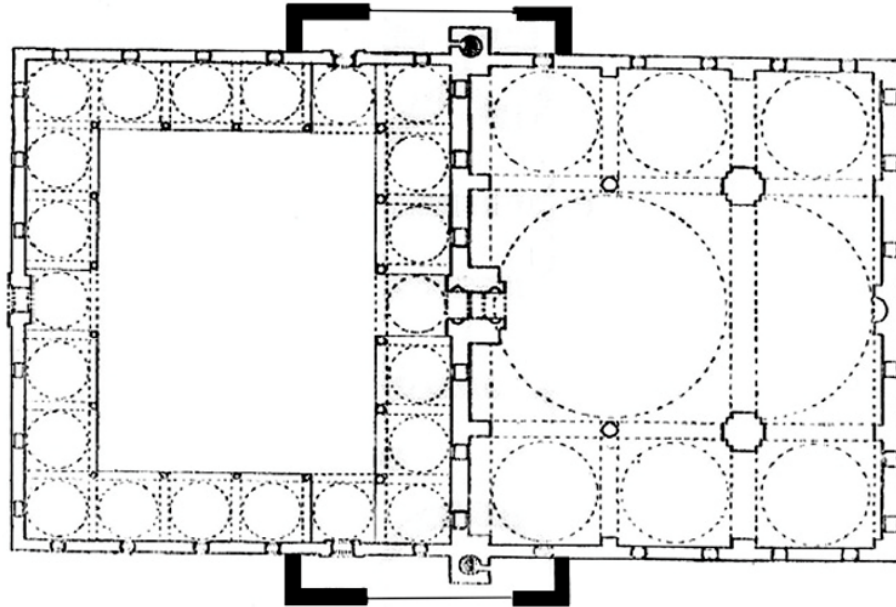


Figure 2.1. Old Mosque's Plan (Ayverdi, 1973)

2.3.2. The New Mosque

The main dome experienced total collapse and all of the walls of the mosque were damaged beyond repair due to the 1766 earthquake. Therefore the architect, Mehmet Tahir built the current mosque on the same foundations but in a different plan under Mustafa III. The construction of the mosque was completed in 1771.

Today, the mosque has a 26-meter diameter main dome and four semi-domes that support the main dome on its four sides. Four small domes are found on the four corners of the square shaped plan of the main structure. The main dome is supported by four main arches and underlying four big marble piers (columns) which also support the semi-domes. The new mosque is slightly wider than the old one and has an architectural layout similar to the classical mosques of the sixteenth century (Figure 2.2) . The general view of the Fatih Mosque can be seen in Figure 2.3.

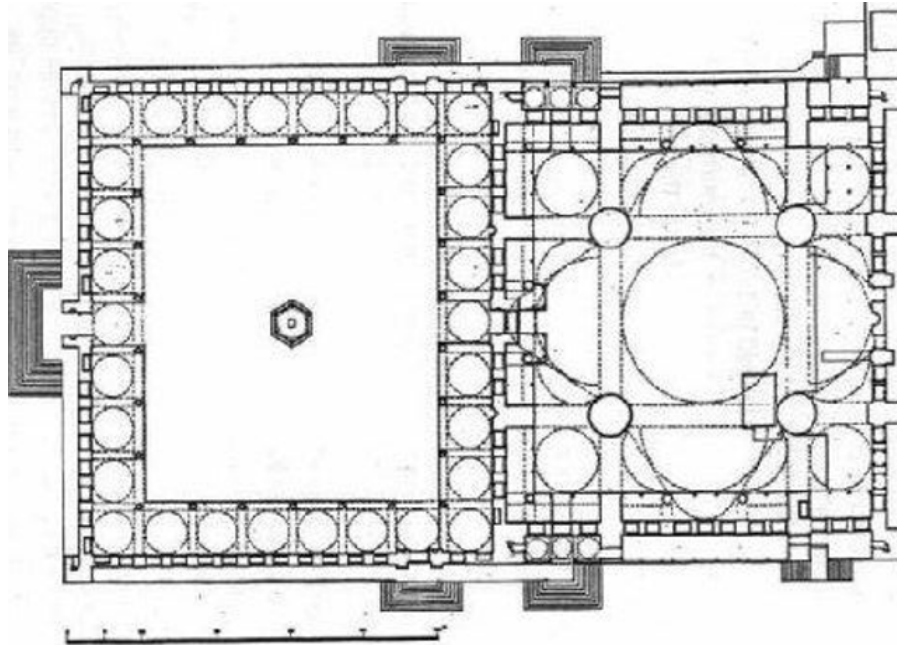


Figure 2.2. New Mosque's Plan (Gurlitt)



Figure 2.3. General View of the Mosque.

2.4. The Restoration of Fatih Mosque Between 2007-2012

Most recent damage to the mosque was induced by the 1999 Kocaeli earthquake. The damages were to such an extent that the structure underwent a restoration and strengthening between 2007 and 2012.

2.4.1. Restoration

The restoration of the Fatih Mosque started in 2007 soon after the Committee IV for Preservation of the Environment and Cultural Heritage approved the building survey, restitution plan and restoration project. The restoration was carried out under the control of the First Regional Directorate for Foundations [11].

Within the scope of restoration works, cracks that were found in all top layers repaired using various methods. There were corroded steel rings and flanks in the

mosque, which were replaced with new original materials whenever applicable. Then, the new material was coated with epoxy based substance. The same method was also repeated for corroded nails, braces and brass rings located on the top and the bottom of columns [11].

The lead layer which protected the mosque's roof had been worn off by environmental factors (rain, wind, bird feces etc.) and was renewed. Moreover, a thick dirt layer on mosque's stone exteriors that had built up due to rain and carbon monoxide gas from vehicle traffic nearby the mosque was cleaned. Additionally, stone surfaces, that were eroded for more than 5 cm deep, were replaced with Kufeki stone that share similar physical attributes with the original stone. Furthermore, dirty, chipped and cracked marble surfaces were cleaned and repaired. The decayed wooden surfaces were reproduced in oak wood and were installed in their original locations. Damaged wooden doors and shutters were repaired [11].

2.4.2. Strengthening

Within the scope of the strengthening works, firstly, the separations in the minaret's stones (Figure 2.4) on the northeastern side of the mosque were joined with a stainless steel clamp (Figure 2.5) and the remaining cracks and openings were filled with a mortar similar to the original [12].

All cracks found in the main dome and in the domes of the porticoes were cleaned by air jet and then repaired by suitable methods according to their width. Losses and breaks were found in the peripheral tie beam at an elevation of approximately +6.00m. Due to excessive corrosion there were reductions in the cross sections of iron circular and linear ties. They were renewed wherever possible to ensure the continuity in the beam. In places with no access for renewal or replacement the new elements were bolted to the old ones [12].

It has been determined that the timber tie beams in the semidomes located at about 1.60 m from their base were cut at places and became dysfunctional over time.



Figure 2.4. Separations in the minaret's stone



Figure 2.5. Application of stainless steel clamp



Figure 2.6. The old peripheral tie beam

This system was replaced with a new tie beam system made of stainless steel. The same process was repeated in four semi-domes and finally the overall continuity was established by connecting the semidomes with adjacent counterweight tower [12].



Figure 2.7. The disfunctional timber tie beams

Lastly, the steel porches on the northeastern and southwestern sides of the mosque have been renewed due to deterioration in members and in adequate supports.

3. METHODOLOGY

3.1. Fatih Mosque Structural Health Monitoring System

The system was installed in 2012 and recorded substantial amount of earthquakes and also the 2016 explosions in Istanbul. The instrumentation consists of 13 accelerometers and 4 tilt meters. Acceleration sensors (Guralp CMG-5T) have three channels and they recorded at 100 Hz in 2013 and have been operating at 200 Hz sampling rate since 2014. The four two-axial tilt meters operate at 50 Hz sampling rate.

The positioning of sensors is crucial for optimum observation of structural behavior and response parameters. The load-bearing system of the mosque consists of four main pillars, four semi-domes, the main dome and the eight piers along the periphery of the main prayer hall that basically support the semi domes. These members of the main structural system were chosen to install the instruments. The monitoring system consists of 13 three-axial accelerometers, recording along X, Y and Z directions. One of them is at the ground level; eight of them are at the gallery level (i.e. a level corresponding to the top of the piers at which the main arches in the case of four interior piers and the four semi domes in the case of external piers spring) and the remaining four are at the dome level. As it can be seen from the plan of the mosque (Figure 3.1), the gallery level has two separate geometrically distinguishable parts. Four gallery level instruments are located on the top of the main piers supporting the main arches and thus the main dome. The remaining four gallery level instruments are positioned midway on the four external walls near the lower extremities of the four semi-domes.

There is one station at the ground level, which is codes as ZEM. The sensors on the main piers are named GAL1, GAL2, GAL3 and GAL4. The mihrab is between piers with stations GAL3 and GAL4. The courtyard is on the opposite side, adjacent to the pillars with stations GAL1 and GAL2. The instruments named GALA, GALB, GALC and GALD are near the lower margins of the semi- domes. The dome base stations are called KUB1, KUB2, KUB3 and KUB4. Similar to other installations

(Hagia Sophia, Süleymaniye etc.), the mihrab direction is where the north channel of instruments is aligned with. The courtyard-mihrab axis we always call X axis. The layout of the monitoring system is shown in Figures 3.1, 3.2, 3.3 and 3.4.

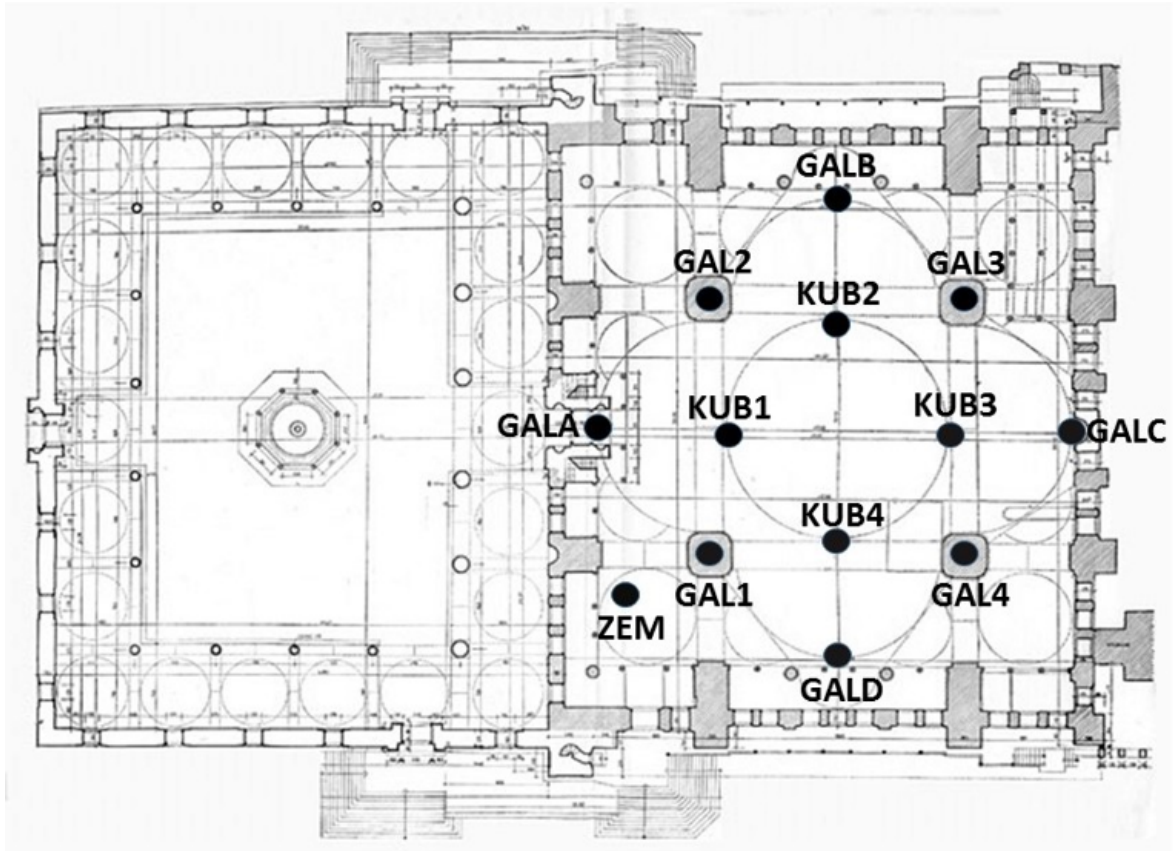


Figure 3.1. Fatih Mosque Structural Health Monitoring System, plan view (Gurlitt)



Figure 3.2. Instrument layout in section, X-axis

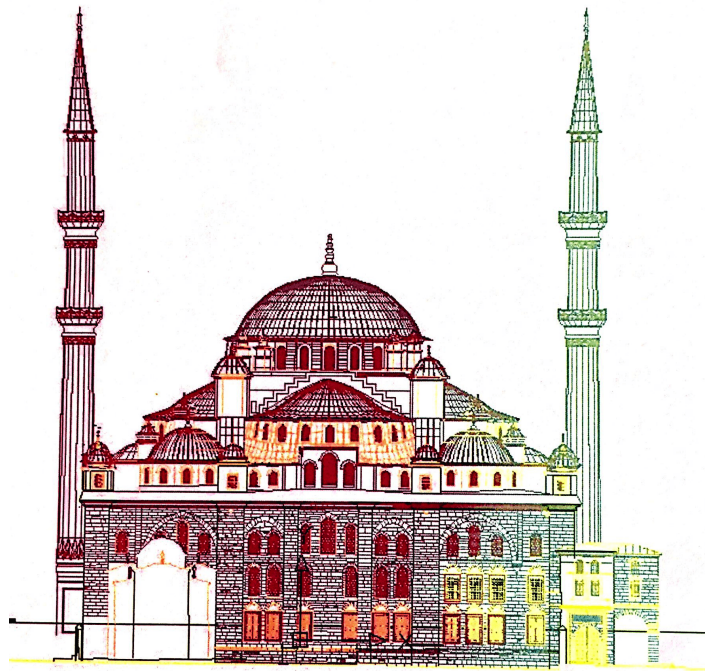


Figure 3.3. Instrument layout in section, Y-axis



Figure 3.4. Fatih Mosque SHM system, interior view (TripAdvisor)

3.2. Earthquake Data

In this study the earthquakes recorded by the Fatih Mosque SHM system in the years between 2013 and 2016 and in the first two months of 2017 are considered.

As Istanbul is located in a high seismicity region, there was sufficient amount of earthquake data to determine the dynamic properties of the mosque. The location of the Fatih Mosque is indicated in Figure 3.5. During the four year period, the mosque experienced more than 160 earthquakes whose magnitudes varied between 2.1 and 6.5 in Richter scale. However, some limitations were applied to the database considering non-recording by all sensors, low signal to noise ratio, distance and magnitude properties. First of all records of earthquakes with a low signal to noise ratio were removed, as for such cases it was not possible to distinguish the signal from natural noise level. Secondly, the events which were not uniformly recorded by all sensors, were excluded. Lastly, only events with epicentral distances smaller than 500 km to the mosque were included in analysis. However if an earthquake had a magnitude 5.5 and above, it

was included in the database regardless of other criteria. These criteria reduced the database to 57 earthquake events, the records of which were considered in this study. Epicenters of these 57 earthquakes recorded in the Fatih mosque are given in Figure 3.6 and 3.7.

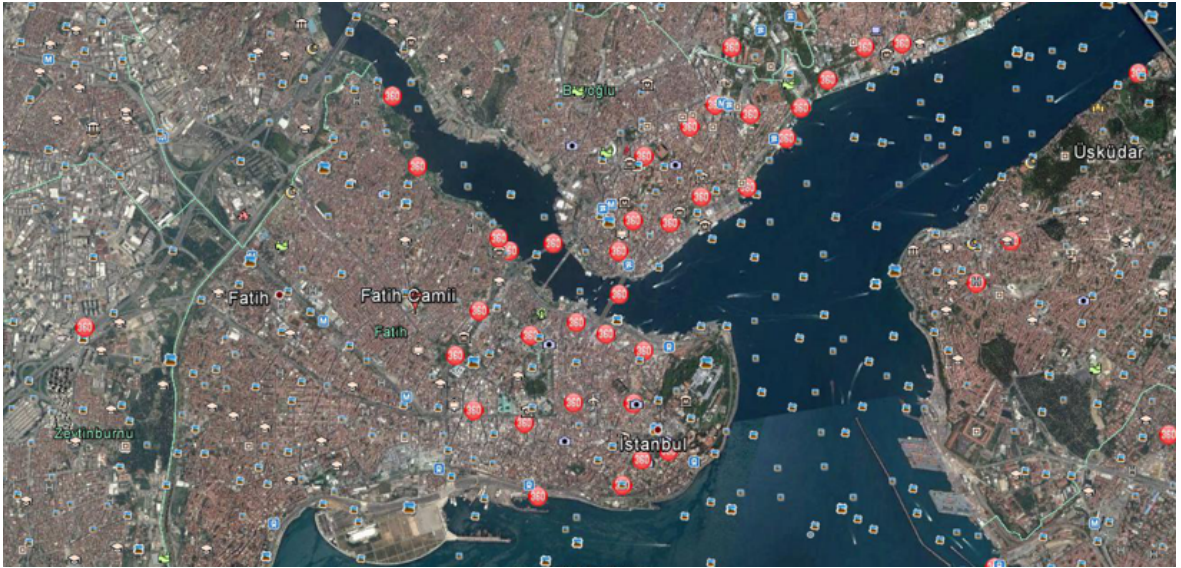


Figure 3.5. General Location of Fatih Mosque (Google Earth).

Histograms of magnitude, distance and azimuth can be seen in Figures 3.8, 3.9 and 3.10. Looking at the magnitude histogram, it can be seen that during the four-year period, the majority of earthquakes had magnitudes in the range between 3 and 4, while earthquakes having magnitudes 2.2 to 3 and 4 to 5.1 occur less often. Number of large earthquakes having magnitudes bigger than 5.0 are considerably small.

Another histogram which is for distance (Figure 3.9) shows that most of earthquakes included in our database took place within 50 km of the Fatih Mosque. There are no events at distances between 400 and 500 km.

The azimuthal map in Figure 3.10 shows the region within 500km of the Fatih Mosque. The histogram (Figure 3.11) displays that the epicenters of earthquakes in the database are mostly between

200 to 275 degrees, which correspond to Aegean Sea and southwest Marmara regions. In contrast, within degrees of 0 to 150 there are only a few events. Consequently, the earthquakes originating mainly from the south-west of the mosque have the majority in the database, while north-easterly and northerly events are considerably less than earthquakes occurring to its general south.

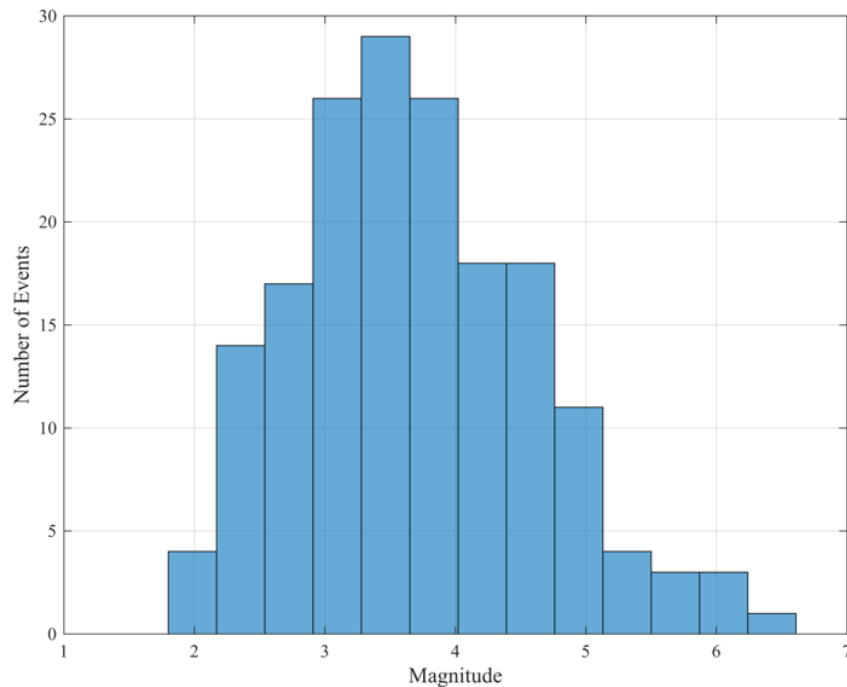


Figure 3.8. Magnitude Histogram.

Another histogram which is for distance shows that most of earthquake in our database come from nearby. Without having a sufficient reason, there is no event distances between 400 and 500 km. In another word, the database almost consists of earthquakes distances below 350 km.

The azimuthal map of Fatih (Figure 3.10) shows the area around Fatih in with 500 km diameter. Histogram displays that the epicenter of earthquakes mostly between 200 to 275 azimuthal degrees, these degrees on azimuthal map corresponds to Aegean Sea region. In contrast, degrees of 0 to 150 is the region that experiences least events.

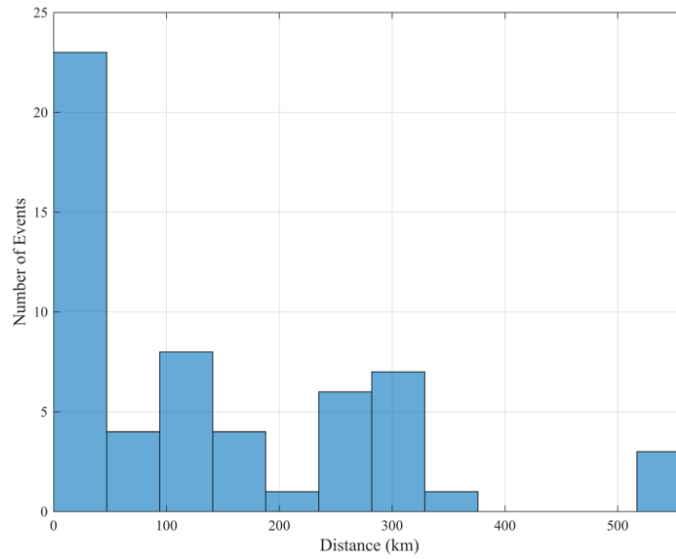


Figure 3.9. Distance Histogram.

Consequently, the earthquakes originates mainly from south-west of the mosque while north-east and north of the mosque experience less earthquakes comparing south-east of the mosque.

Epicentral properties of the events in the database and corresponding peak ground accelerations at the ground level station ZEM are given in Tables 3.1, 3.2 and 3.3. It was observed that the occurred peak in X or Y direction depends on the epicenter of the event. More clearly, if the epicenter is in south-east of the mosque it gives higher amplitude in same direction that we call Y direction.

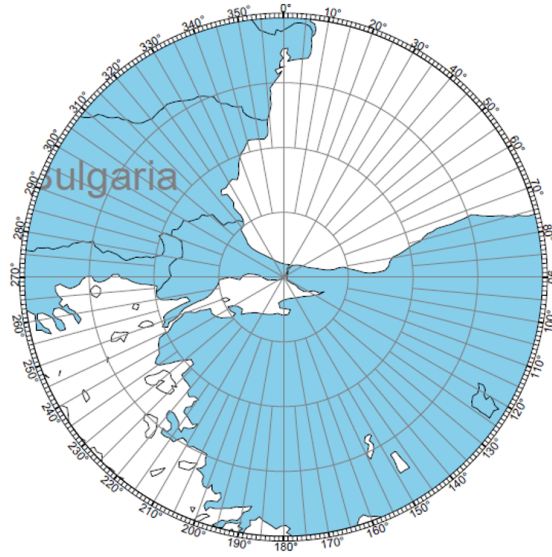


Figure 3.10. Azimuthal Map.

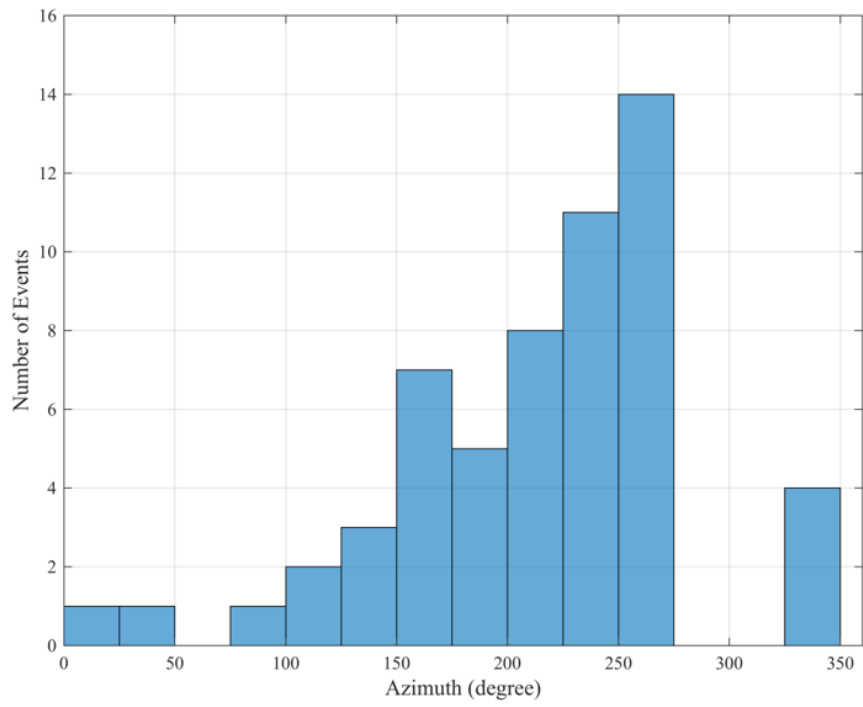


Figure 3.11. Azimuthal Histogram.

The largest earthquake recorded by the system occurred on 24 May 2014 in the Northern Aegean Sea, having 6.5 magnitude and 303 km epicentral distance. This and following five earthquakes with the largest PGA's have been chosen for use in the detailed modal analysis. Peak accelerations in the 6.5 Aegean earthquake reached 0.014 g.

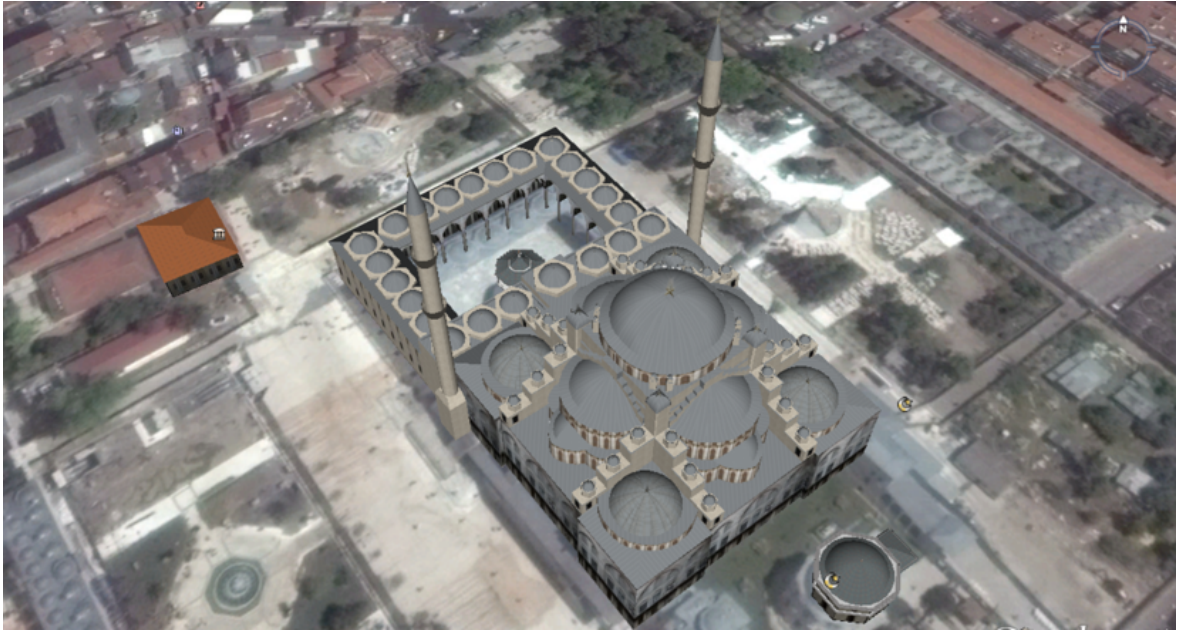


Figure 3.12. Azimuthal Location of Fatih Mosque (Google Earth)

3.3. Data Processing

Analysis of seismic records is based on three main steps; data processing, system identification and interpretation. Data processing is carried out for removing the noise in the records by using filtering, base-line correction and instrument correction. System identification is basically used to determine dynamic characteristics of a system from its recorded dynamic response by using techniques such as Fourier analysis.

With the developments in computer technology in the last decades more and more structures have been instrumented with seismic monitoring systems. As a result enormous amounts of earthquake data have been accumulated. Yet these raw data are not proper to use directly in analysis.

These digital signals need to be processed to minimize the noise in the records resulting from instruments or other unwanted ambient signals in the recording environment.

Using techniques of system identification, structural modal properties can be estimated. It is also possible to identify particular response characteristics such as rocking torsional and soil-structure interaction. Damage detection is mostly related to nonlinear behavior in the structure. The conventional way to detect damage is to detect the frequency changes in the structure. However, global frequencies are not that sensitive to changes in local frequencies. Therefore, wave propagation techniques may be a more rational way for damage identification and detection.

3.3.1. Filtering

Band-pass filter eliminates the components of a record outside the filtering range. All modes of vibration should be within this frequency range. The low corner frequency is best determined with the help of displacement time histories of recordings. Because displacement time histories are obtained by double integrating the acceleration time histories the noise induced errors are larger in displacement time histories. When applying band-pass filter an important point is to avoid changes in the phase content of the original record. Zero- phase filters or filtering the signal twice first forward and then backward minimize the phase changes. For the high corner frequency a frequency that includes all significant structural modes should be selected, which is generally below 20 Hz in buildings. In this study, the low corner frequency determined as 0.5 Hz and the high corner frequency determined as 20 Hz.

3.3.2. Smoothing

Noise can create imaginary high amplitude peaks in the spectra. Smoothing reduces the noise effect in Fourier spectra. Smoothing window should be neither too short to be effective nor too long to cause loss in real peaks. In this study, the process suggested in Safak (1997) is used to select the optimal window length.

Table 3.1. Earthquakes recorded between 2013 (Jan) and 2014 (June) in Fatih Mosque

Event Date (dd.mm.yy)	Time (Local)	Event Coordinates		Depth (km)	Event Location	Magnitude (ML)	Distance (km)	Azimuth (degree)	Acceleration (cm/sn ²)		
		Longitude	Latitude						Zem X	Zem Y	Zem Z
8.1.2013	16:06:06	39.6462	25.4833	8.4	Aegean Sea	6.2	330.5	243.668			
27.3.2014	20:20:08	41.0095	28.3462	8.4	Marmara Sea	2.9	50.6	268.930	0.123	0.084	0.069
7.4.2014	04:25:45	40.8727	28.7187	20.7	Avcılar (Istanbul)	2.5	25.3	230.004	0.051	0.058	0.135
7.4.2014	12:51:02	41.1043	28.8817	5.2	Sultangazi (Istanbul)	2.1	11.0	328.779	0.052	0.080	0.087
17.4.2014	12:55:27	40.7995	27.7697	6.5	Marmara Sea	3.2	102.0	256.526	0.047	0.056	0.050
24.5.2014	12:25:01	40.3242	25.4687	23.3	Aegean Sea	6.5	303.0	256.384	14.424	11.693	7.828
24.5.2014	13:11:40	40.3892	26.1418	9	Saros Gulf	4.3	246.4	254.423	0.113	0.113	0.093
24.5.2014	13:35:00	40.4247	26.1357	1.3	Saros Gulf	4.1	245.8	255.336	0.051	0.044	0.052
24.5.2014	14:33:07	40.284	25.6083	4.9	Aegean Sea	4.7	293.0	254.913	0.203	0.176	0.120
24.5.2014	17:49:14	40.4013	25.9517	2.1	Saros Gulf	4.6	261.4	255.762	0.087	0.107	0.046
25.5.2014	14:38:38	40.4235	26.1442	13.1	Saros Gulf	4.8	245.1	255.259	1.080	1.258	0.520
25.5.2014	14:47:55	40.4103	26.0895	6.8	Saros Gulf	4.5	250.0	255.239	0.151	0.159	0.107
28.5.2014	06:59:51	40.422	26.14	13.3	Saros Gulf	4.5	245.5	255.245	0.164	0.203	0.113
22.11.2014	21:14:15	45.742	27.2147	27.9	Romania	5.6	542.5	345.639	0.914	1.031	0.464
23.11.2014	04:30:06	39.3512	29.018	5.3	Simav (Kütahya)	4.5	185.3	178.191	0.291	0.340	0.175
6.12.2014	03:45:06	38.8942	26.2723	12.4	Aegean Sea	5.1	327.9	224.866	0.795	0.777	0.207
6.12.2014	08:20:53	38.8955	26.2693	13.4	Aegean Sea	5	328.0	224.917	0.397	0.414	0.175
6.12.2014	18:08:28	40.7382	29.048	5	Çınarcık (Yalova)	2.6	32.3	165.195	0.152	0.072	0.169
6.12.2014	18:18:39	40.7545	29.02	3.4	Çınarcık (Yalova)	2.4	30.0	168.665	0.069	0.039	0.062

Table 3.2. Earthquakes recorded between 2014 (Dec) and 2015 (May) in Fatih Mosque

Event Date (dd.mm.yy)	Time (Local)	Event Coordinates		Depth (km)	Event Location	Magnitude (ML)	Distance (km)	Azimuth (degree)	Acceleration (cm/sn ²)		
		Longitude	Latitude						Zem X	Zem Y	Zem Z
16.12.2014	11:02:13	40.1478	27.0735	8.8	Biga (Çanakkale)	4.4	185.4	239.156	0.419	0.384	0.193
19.12.2014	19:57:14	40.7882	28.8098	7.9	Marmara Sea	2.1	28.2	204.630	0.040	0.045	0.033
20.12.2014	00:56:00	40.8138	28.8165	5.4	Marmara Sea	2.4	25.4	206.135	0.063	0.063	0.046
22.12.2014	03:44:00	40.7453	28.715	5.4	Marmara Sea	2.4	36.3	212.995	0.060	0.039	0.039
24.12.2014	02:21:18	40.3635	27.742	6.9	Erdek Gulf	3.2	125.0	234.778	0.041	0.045	0.035
29.12.2014	10:06:22	38.8902	26.277	12.1	Aegean Sea	4.5	328.0	224.762	0.291	0.182	0.076
30.12.2014	01:25:59	40.8437	28.8525	10.9	Marmara Sea	2.4	21.2	202.727	0.112	0.098	0.052
17.1.2015	02:42:34	39.8848	30.3955	5.5	Tepebaşı (Eskişehir)	4.3	175.4	135.419	0.239	0.297	0.074
19.1.2015	13:10:43	40.8648	28.6787	16	Marmara Sea	3	28.5	233.011	0.156	0.148	0.180
22.1.2015	18:47:34	40.6233	29.1082	12.3	Çınarcık (Yalova)	2.5	46.0	163.125	0.036	0.028	0.045
1.2.2015	12:46:31	40.7125	27.4973	6	Tekirdağ (Marmara Sea)	3.5	126.6	254.858	0.113	0.096	0.089
6.2.2015	01:41:22	40.663	29.1637	11.6	Çınarcık (Yalova)	3	43.5	155.527	0.264	0.176	0.119
6.2.2015	13:32:10	40.7163	29.127	9.8	Çınarcık (Yalova)	3	36.8	156.112	0.397	0.193	0.188
8.3.2015	22:43:58	40.8547	28.6942	8.1	Marmara Sea	2.6	28.2	229.595	0.055	0.056	0.056
9.3.2015	00:29:44	40.8502	28.712	8.1	Marmara Sea	2.1	27.4	226.770	0.018	0.016	0.018
22.3.2015	21:48:21	40.847	28.6792	8.1	Marmara Sea	2.4	29.7	229.923	0.054	0.041	0.045
23.4.2015	13:04:19	39.9992	28.7397	3.7	Mustafakemalpaşa (Bursa)	3.5	114.6	188.968	0.051	0.053	0.082
29.4.2015	17:40:53	42.0393	29.3078	14.1	Black Sea	4	117.0	14.605	0.593	0.477	0.344
11.5.2015	07:16:27	40.4148	29.126	7.5	Gemlik (Bursa)	3.9	68.7	167.494	0.486	0.350	0.374

Table 3.3. Earthquakes recorded between 2015 (May) and 2017 (Feb) in Fatih Mosque

<i>Event Date</i> (dd.mm.yy)	<i>Time</i> (Local)	<i>Event Coordinates</i>		<i>Depth</i> (km)	<i>Event Location</i>	<i>Magnitude</i> (ML)	<i>Distance</i> (km)	<i>Azimuth</i> (degree)	<i>Acceleration (cm/sn²)</i>		
		<i>Longitude</i>	<i>Latitude</i>						<i>Zem X</i>	<i>Zem Y</i>	<i>Zem Z</i>
16.5.2015	08:57:16	40.8685	28.2215	13.2	Istanbul (Marmara Sea)	2.8	63.3	254.883	0.098	0.100	0.059
20.5.2015	01:47:16	40.7815	28.837	5.4	Marmara Sea	2.6	28.1	199.750	0.218	0.265	0.159
20.5.2015	03:14:10	40.7962	28.8223	6.8	Marmara Sea	2.3	27.0	203.385	0.092	0.107	0.060
23.5.2015	04:15:57	40.912	28.707	17.4	Avcılar (Istanbul)	2.1	23.6	239.681	0.020	0.017	0.019
1.6.2016	00:14:10	40.8582	28.2177	13.2	Silivri	3.3	64.0	253.973	0.145	0.090	0.096
10.6.2016	00:08:58	40.8553	29.2868	5.4	Pendik(Istanbul)	2.4	33.6	122.729	0.063	0.108	0.050
23.6.2016	02:35:59	40.7062	29.2128	9.9	Yalova	3.6	41.2	147.517	1.160	0.480	0.306
25.6.2016	08:40:11	40.7032	29.2147	6.8	Yalova	4.4	41.6	147.576	5.688	2.395	2.086
17.7.2016	11:55:41	40.7118	29.1800	7.4	Yalovqa	4.0	39.2	150.438	1.627	2.450	1.358
2.9.2016	22:24:57	40.7097	30.1263	9.0	Kartepe (Kocaeli)	3.7	104.6	108.818	0.202	0.174	0.148
24.9.2016	02:11:18	45.7470	26.6192	103.8	Romania	5.8	557.3	341.081	0.424	0.476	0.233
12.10.2016	02:42:43	40.6102	28.9497	5.4	Çınarcık (Yalova)	3.2	45.4	180.017	0.187	0.125	0.145
15.10.2016	11:18:32	42.2063	30.7133	11.4	Black Sea	5.0	196.9	47.427	0.825	1.025	0.434
16.10.2016	17:11:23	40.8993	30.9040	5.0	Cumayeri (Düzce)	3.8	164.3	94.019	0.109	0.145	0.130
25.10.2016	00:04:47	39.7950	28.6703	8	Mustafakermalpaşa (Bursa)	4.1	138.0	189.952	0.206	0.199	0.197
26.10.2016	17:10:31	40.8648	27.8273	5.0	Marmara Sea	3.0	95.7	260.023	0.054	0.071	0.052
28.12.2016	02:20:57	45.3533	26.5457	49.7	Romania	5.9	518.8	338.793	0.402	0.813	0.213
6.2.2017	13:58:00	39.5098	26.0747	6.8	Gülpınar(Çanakkale)	5.3	295.6	236.401	0.707	0.700	0.385
7.2.2017	05:24:02	39.5212	26.0873	5	Gülpınar(Çanakkale)	5.3	294.0	236.480	0.605	0.719	0.437

4. EARTHQUAKE RESPONSE

4.1. TIME DOMAIN CHARACTERISTICS

The chosen 57-earthquakes are analyzed in time domain and their characteristics are shown. The data processing explained in the previous section in details. The filtered acceleration, velocity and displacement time histories of the biggest earthquake that is 6.5 Aegean Sea occurred on 24 May 2014 and 4.4 Yalova occurred on 25 June 2016 are presented in Figure 4.1, 4.2, 4.3, 4.4, 4.5 and 4.6. These two earthquakes were recorded by all stations and had the biggest amplitudes. Despite the 6.2 Aegean Sea earthquakes has the second biggest magnitude and amplitude, the ZEM station could not record it due to some technical problems.

The observation mentioned before is that the difference of magnitudes of peak values between two directions strongly depend on the location of the earthquake. The mosque is located toward kiblah and if an earthquake is coming from southwest or northwest, which is relatively parallel to the Y direction of the mosque, the magnitudes in Y direction is bigger than that X direction. Similarly, when earthquakes comes from southwest or northwest it causes higher amplitudes in X direction.

Figures 4.7, 4.8, 4.9, 4.10, 4.11, 4.12 shows the peak values recorded by all stations. The response in stations at dome level have the highest peaks, yet it can be seen that the response of GALC, GALB and GALD have the highest value in 6.5 Aegean Sea earthquake.

More detailed investigation carried out by comparing the peak ground accelerations, velocities and displacements with magnitudes. It is used the geometric mean of two-sided values of peak ground accelerations, velocities and displacements. Looking at the Figure 4.13, 4.14 and 4.15 the noticeable result is that there is moderate correlation between the magnitude and response.

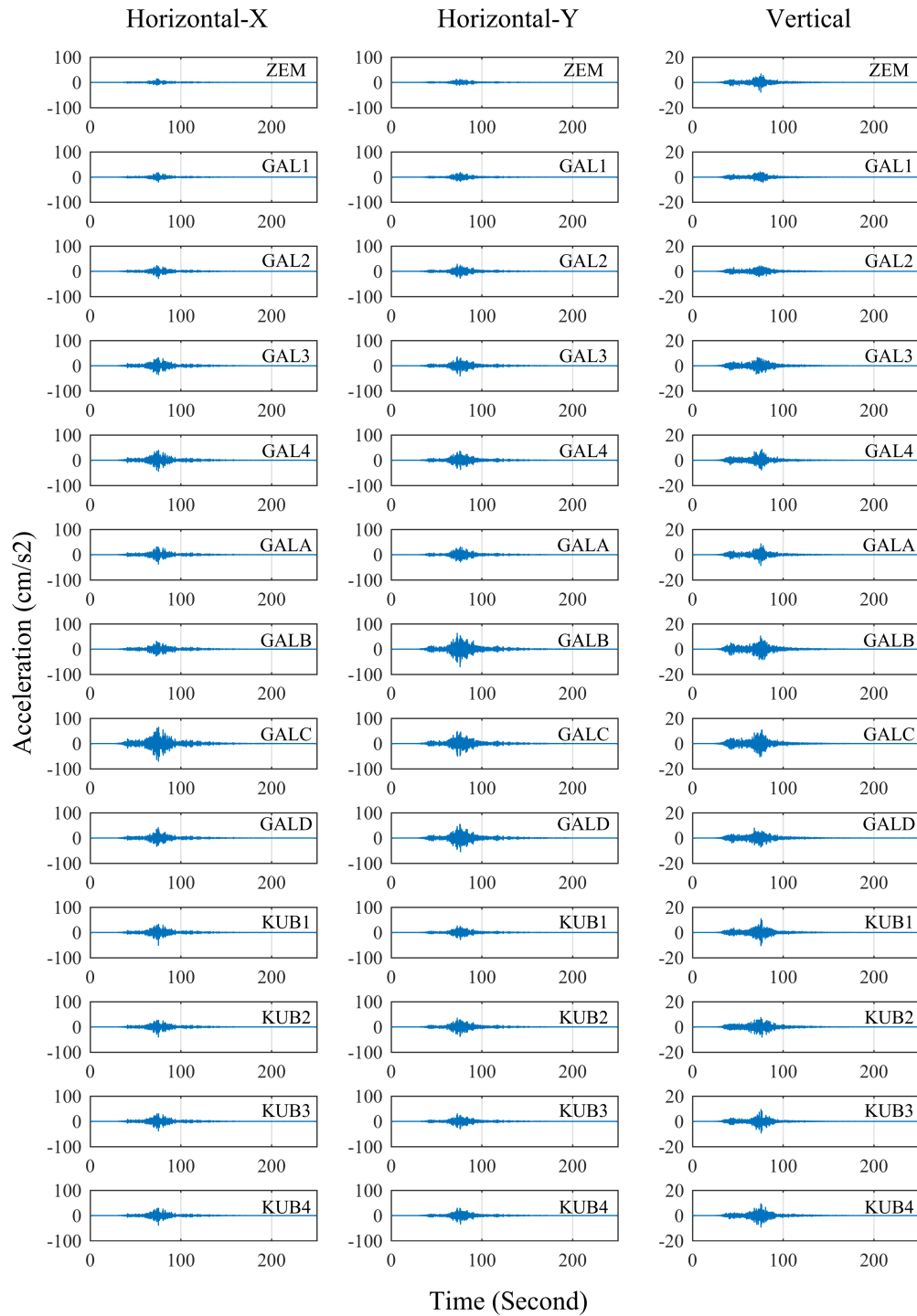


Figure 4.1. Acceleration time history of 6.5 Aegean Sea earthquake

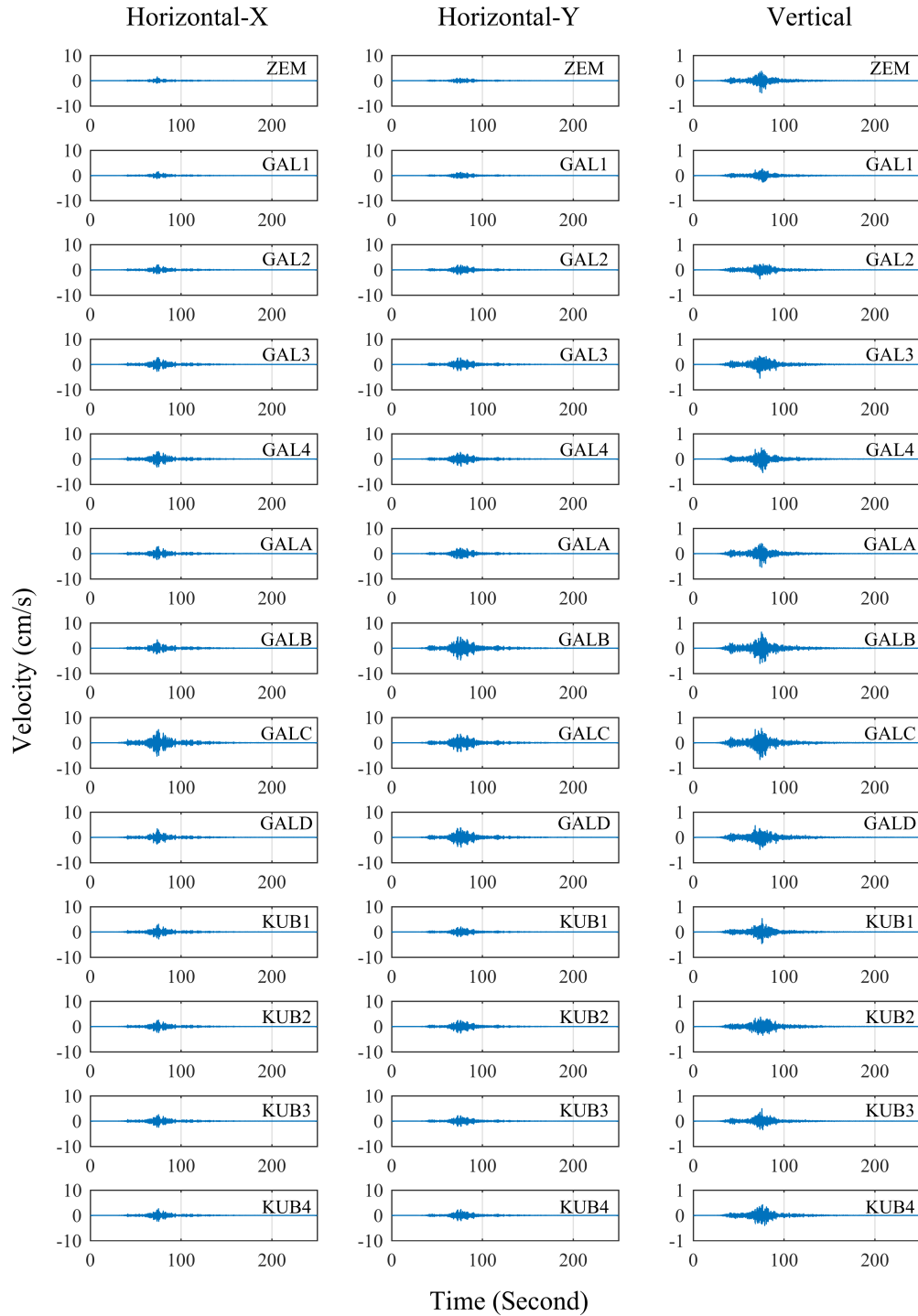


Figure 4.2. Velocity time history of 6.5 Aegean Sea earthquake

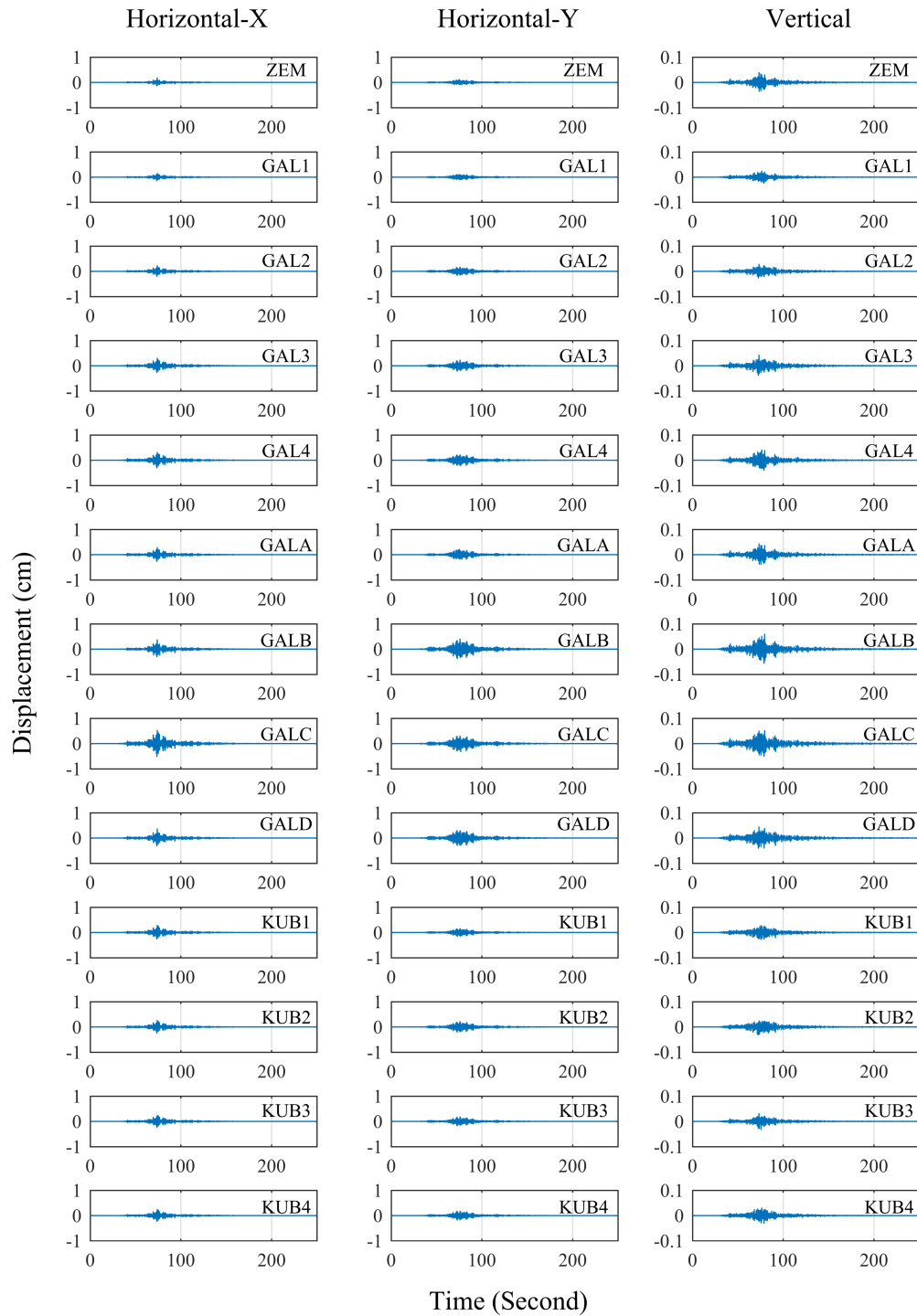


Figure 4.3. Displacement time history of 6.5 Aegean Sea earthquake

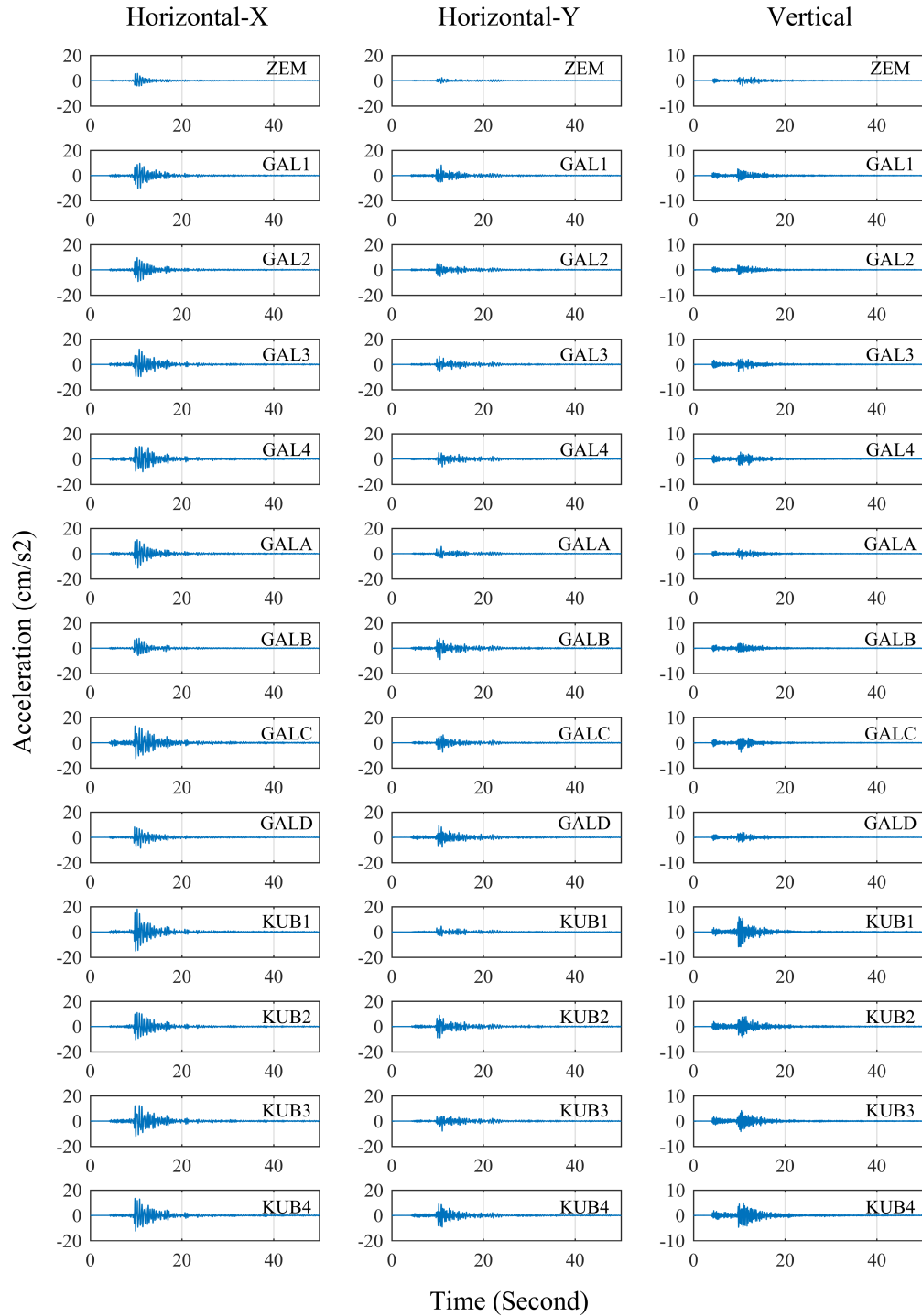


Figure 4.4. Acceleration time history of 4.4 Yalova earthquake

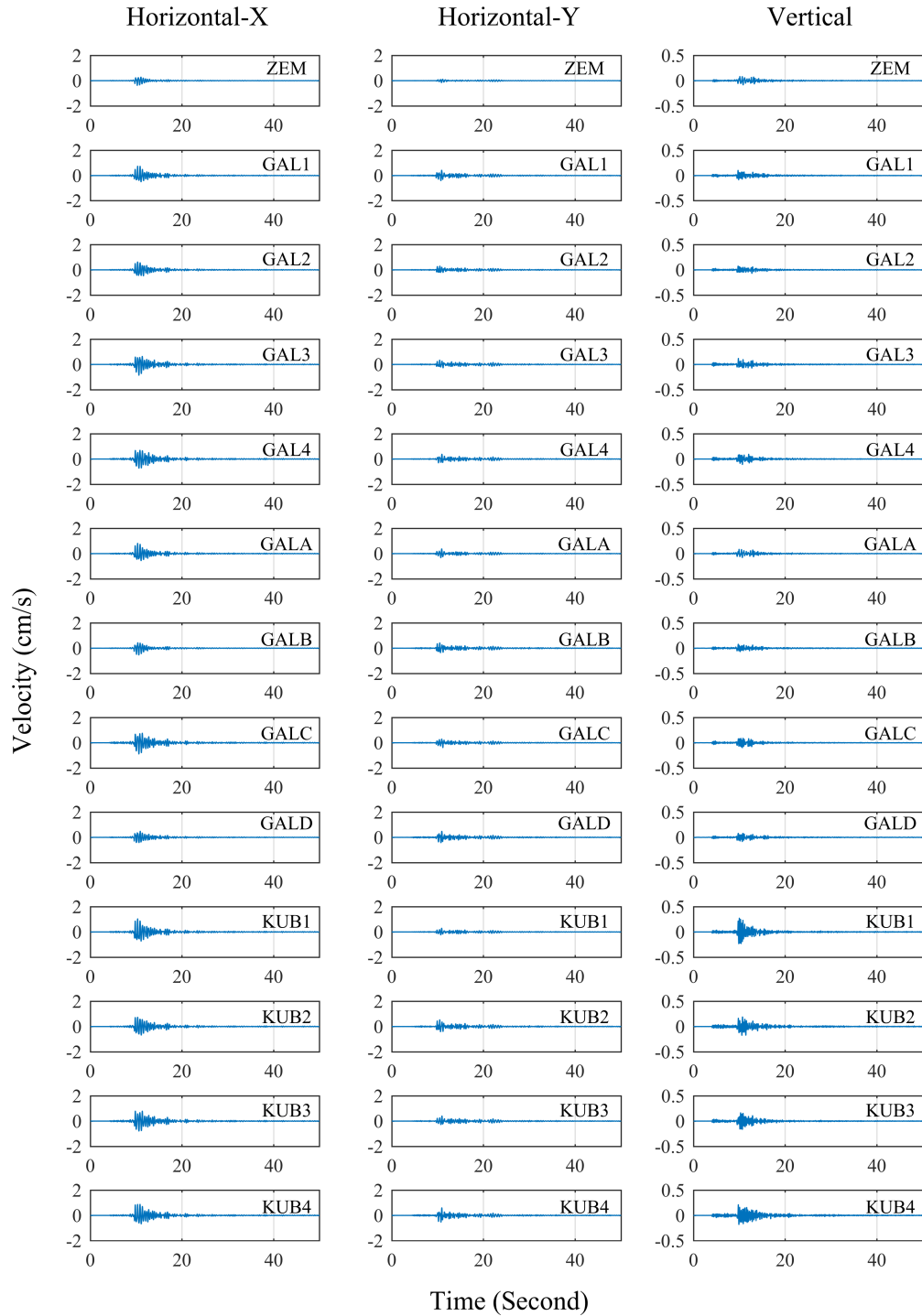


Figure 4.5. Velocity time history of 4.4 Yalova earthquake

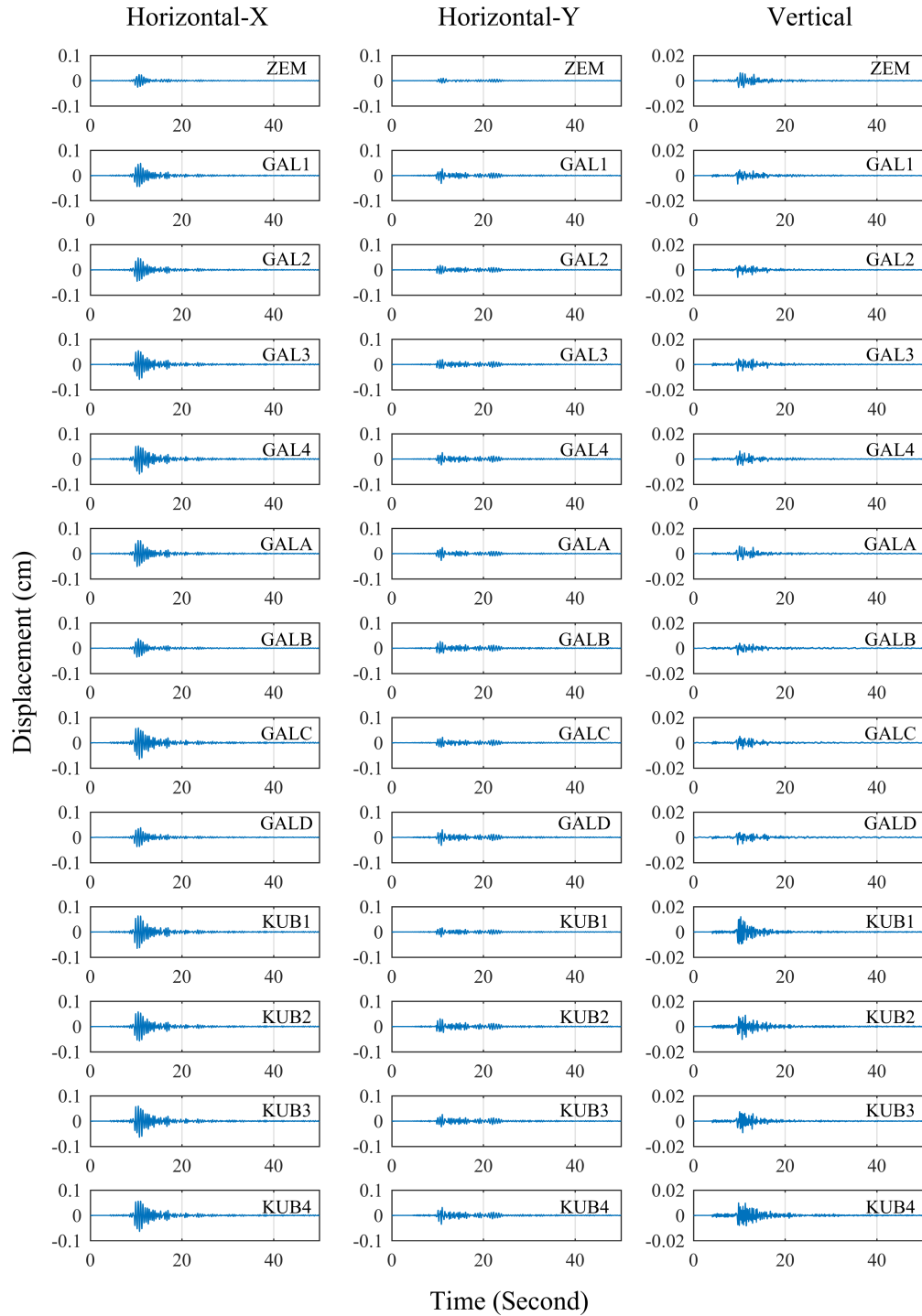


Figure 4.6. Displacement time history of 4.4 Yalova earthquake

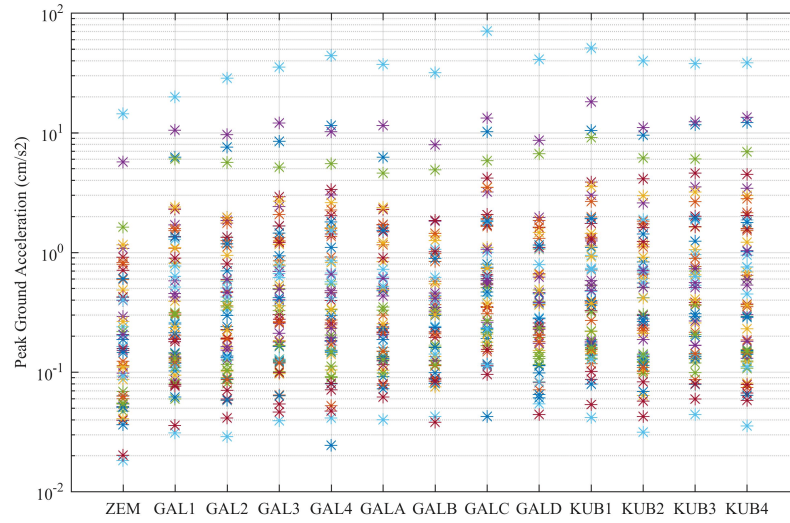


Figure 4.7. Peak Horizontal accelerations in X direction recorded at Fatih Mosque

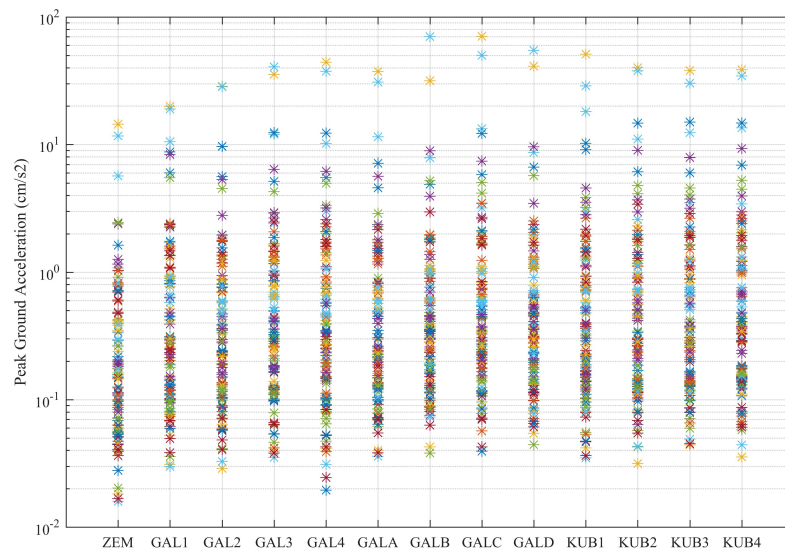


Figure 4.8. Peak Horizontal accelerations in Y direction recorded at Fatih Mosque

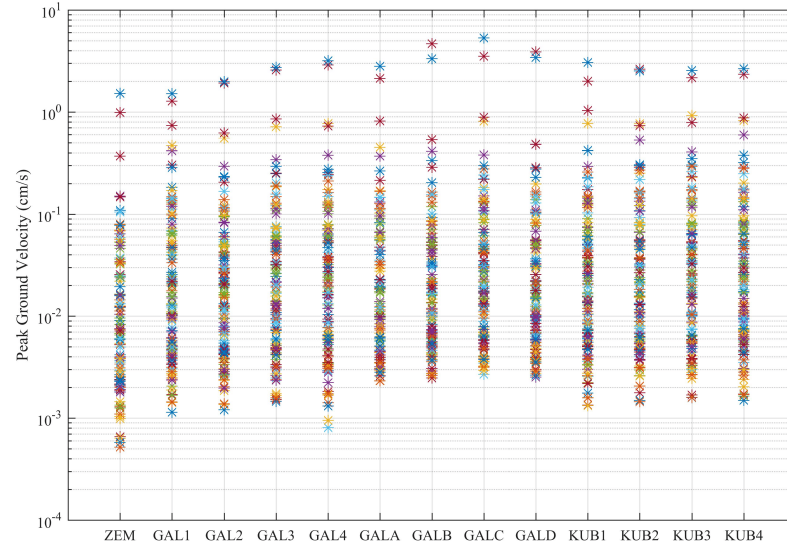


Figure 4.9. Peak Horizontal velocities in X direction recorded at Fatih Mosque

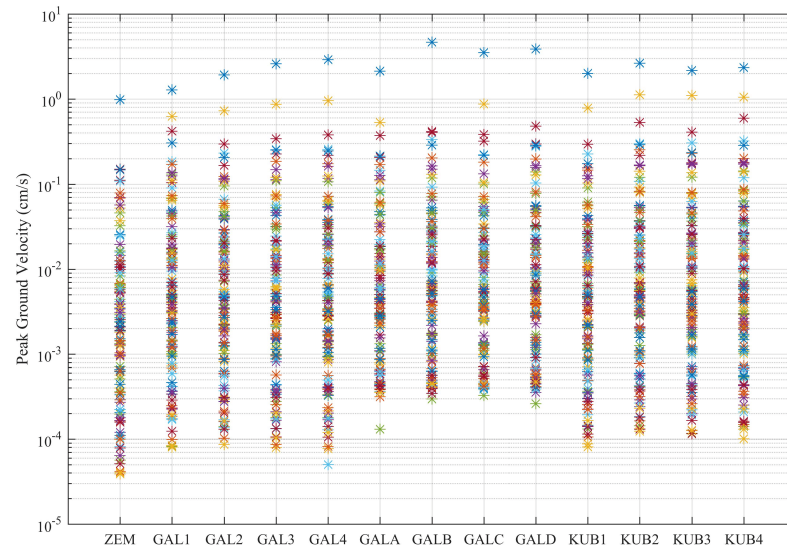


Figure 4.10. Peak Horizontal velocities in Y direction recorded at Fatih Mosque

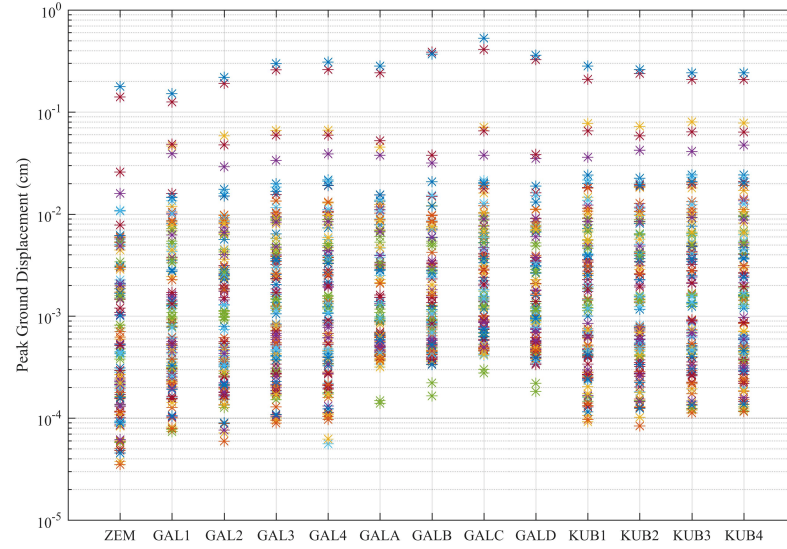


Figure 4.11. Peak Horizontal displacements in X direction recorded at Fatih Mosque

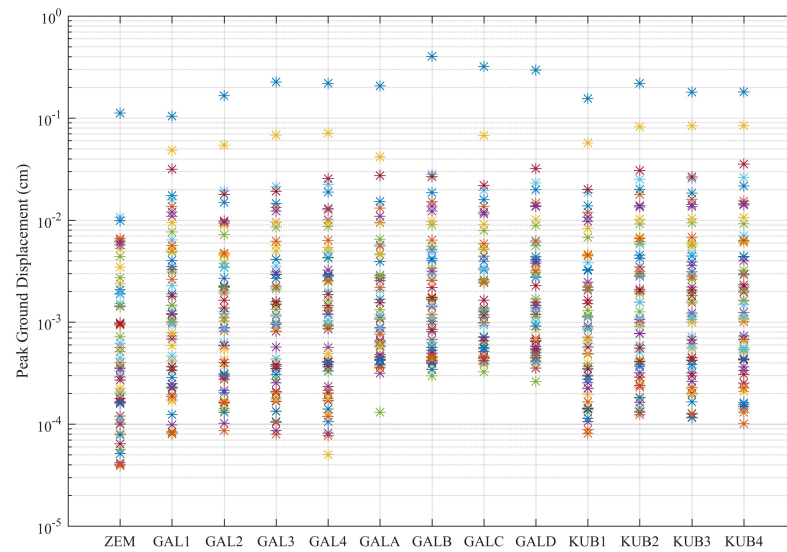


Figure 4.12. Peak Horizontal displacements in Y direction recorded at Fatih Mosque

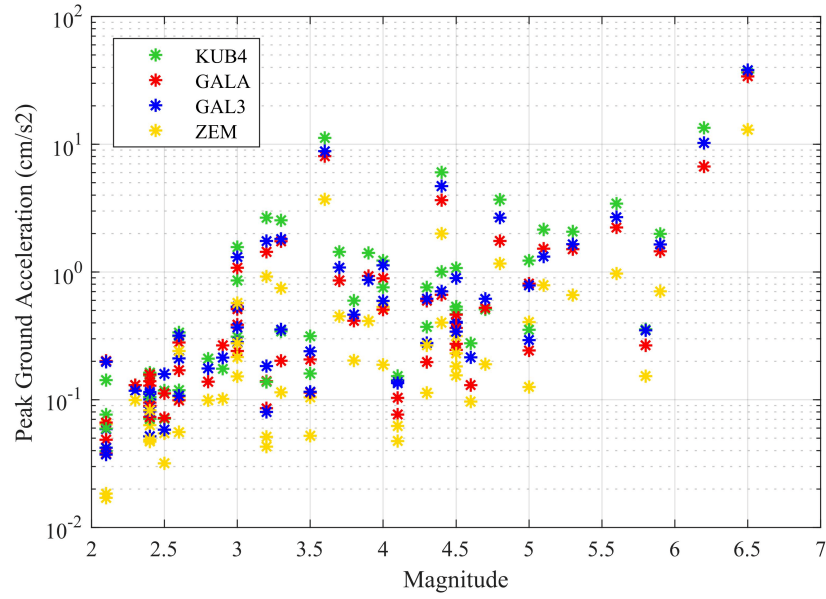


Figure 4.13. Peak Ground Acceleration vs Magnitude

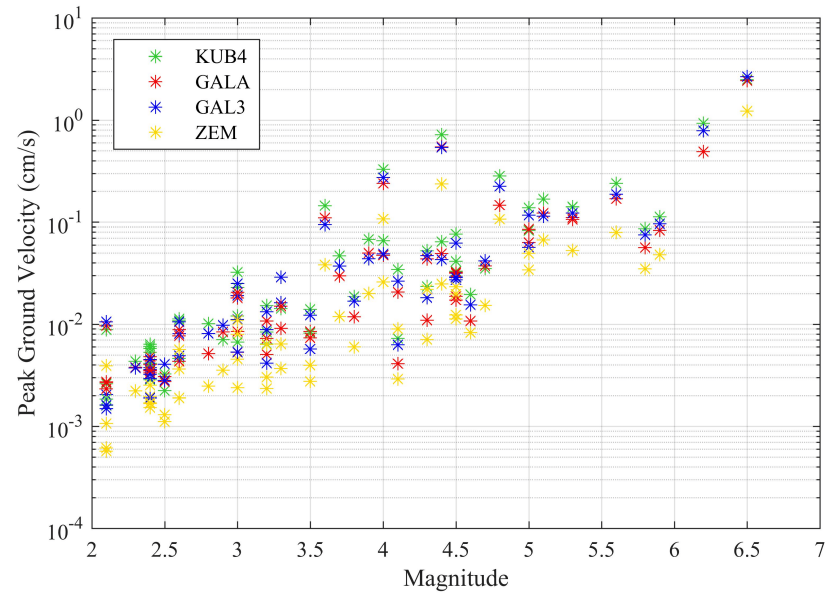


Figure 4.14. Peak Ground Velocity vs Magnitude

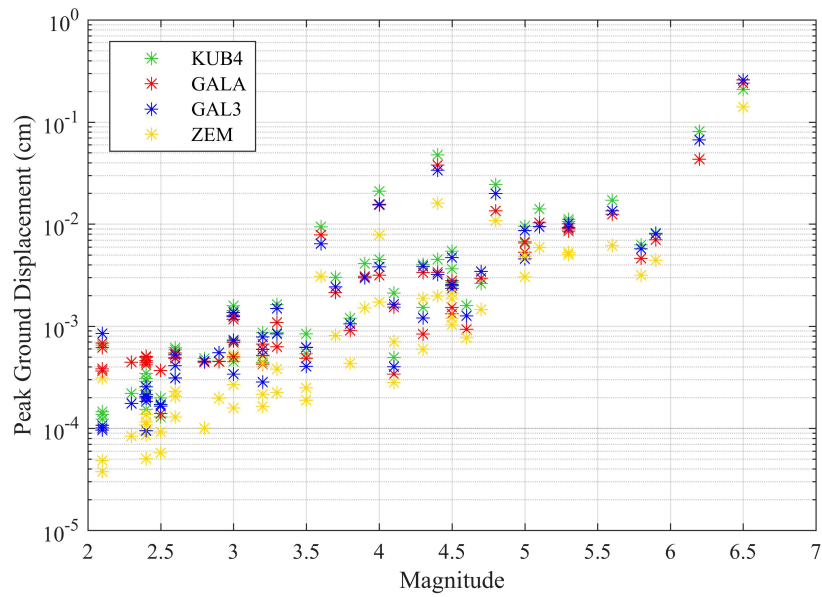


Figure 4.15. Peak Ground Displacement vs Magnitude

4.2. Frequency Domain Characteristics

In modal analysis, we used M6.5 Aegean Sea, M5.6 Romania, M4.4 Yalova, and M4.0 Yalova and M5.0 Black Sea earthquakes. These earthquakes have the largest peak ground accelerations.

4.2.1. Modal Frequencies

The natural frequency we obtain from modal analysis is the one of fundamental parameters to define dynamic response of a structure. Modal frequencies can best be identified from Fourier amplitude spectra of earthquake data. However, as in our case the mosque is subjected to SSI, the fundamental frequencies will be identified from top-to-basement transfer functions.

Transfer functions of the M6.5 Aegean Sea and M5.0 Black Sea earthquakes in two horizontal axes, X and Y are illustrated in Figures 4.16, 4.17, 4.18 and 4.19.

Table 4.1. Modal Frequencies

	Mode 1	Mode 2	Mode 3	Mode 4	Mode 5
Frequencies	2.45	2.74	3.52	5.6	8.1

The response of the mosque is rather complicated and needed to be analyzed in detail for each record set. Identified first five modal frequencies are given in Table 4.1.

Structural behavior in nonlinear range results in decrease in stiffness and consequently increase in natural period. In contrast strengthening indicates an increase in stiffness, that means a decrease in the natural period and increase in natural frequency. There are two studies before restoration and strengthening works of the Fatih Mosque. In the study carried out by Beyen (2007) the first and second modal frequencies are estimated as 2.31 Hz and 2.42 Hz using and analyzing five minute ambient vibration data. The other study performed by a PhD student in 2006 finds that the fundamental frequency of the mosque is about 2.5 Hz in two directions estimated using one hour long data. In our study the first modal frequency is identified as 2.45 Hz and the second as 2.74 Hz. Our results suggest that the increase in the natural frequency could be correlated with restoration and retrofitting works.

It should be kept in mind that estimates of two previous studies are based on ambient vibrations which are low level and during which the structure is expected to respond in the linear range. Our estimations on the other hand are based on records of largest amplitudes in our data set and are very likely already include frequency reduction due to nonlinear response.

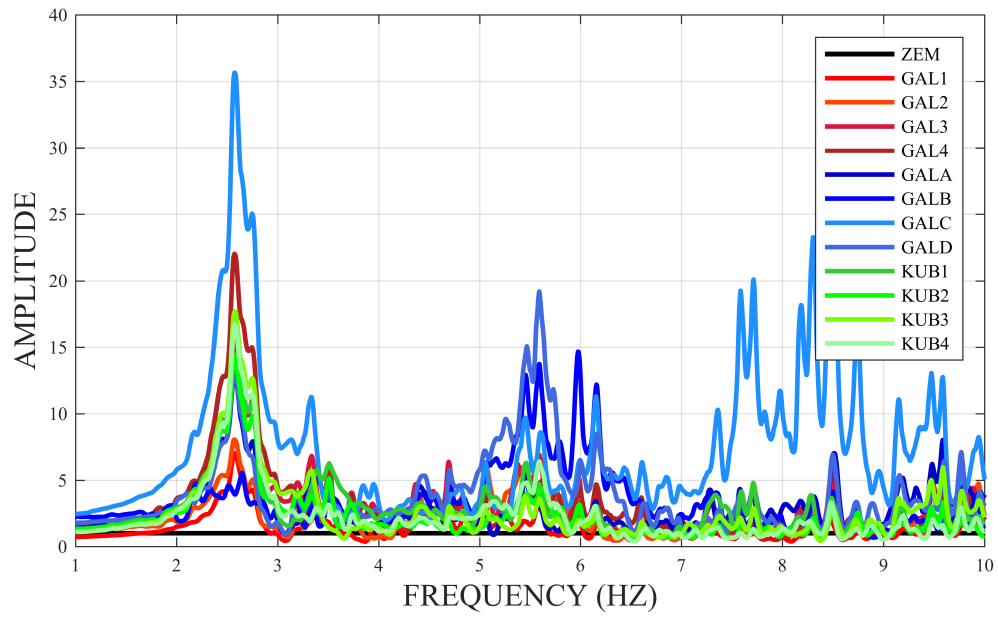


Figure 4.16. Horizontal (X) top-to-basement Transfer Function of 6.5 Aegean Sea earthquake

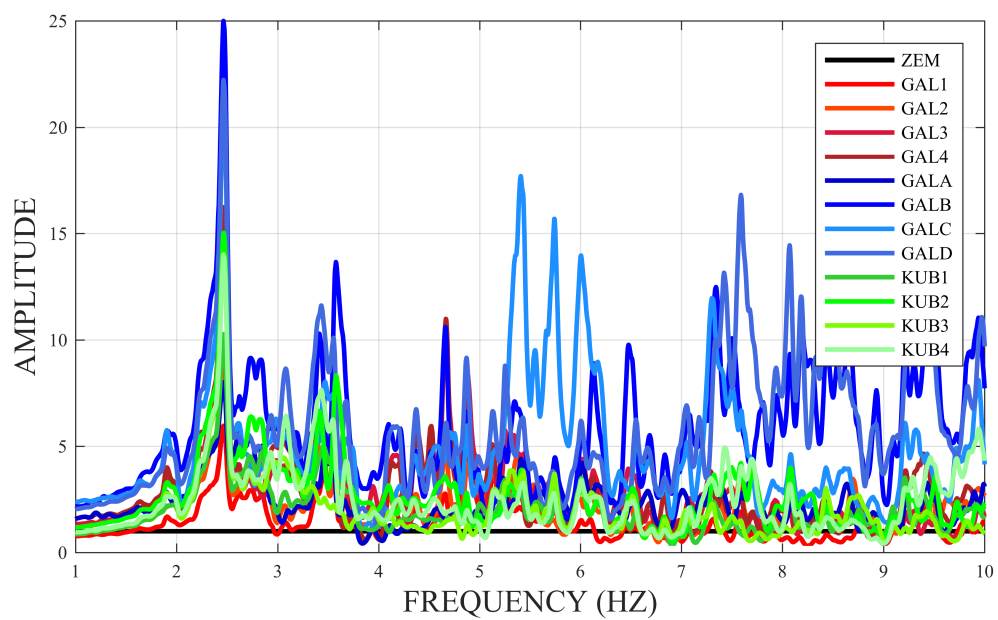


Figure 4.17. Horizontal (Y) top-to-basement Transfer Function of 6.5 Aegean Sea earthquake

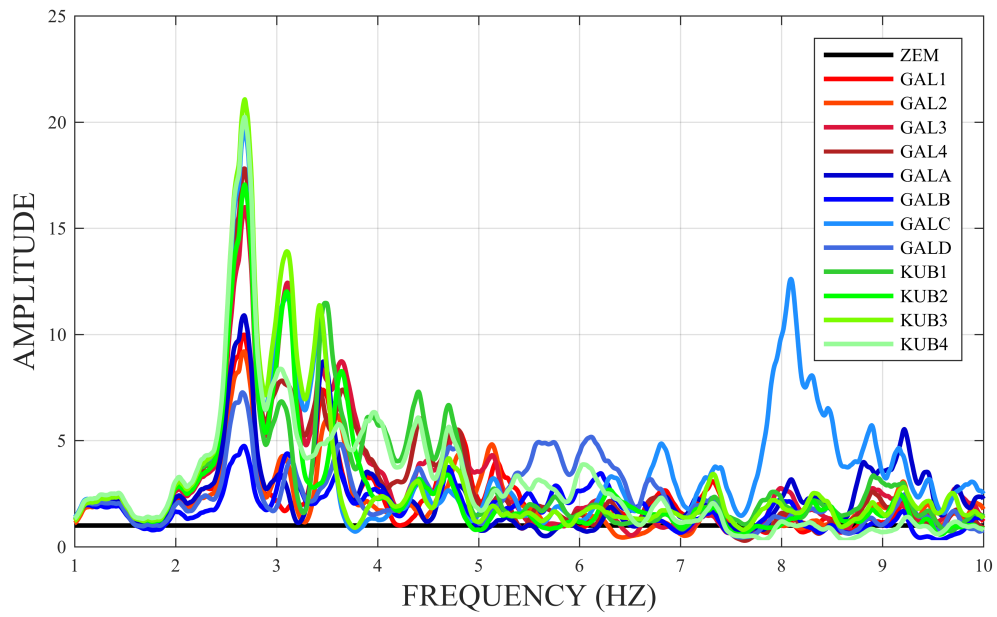


Figure 4.18. Horizontal (X) top-to-basement Transfer Function of 5.0 Black Sea earthquake

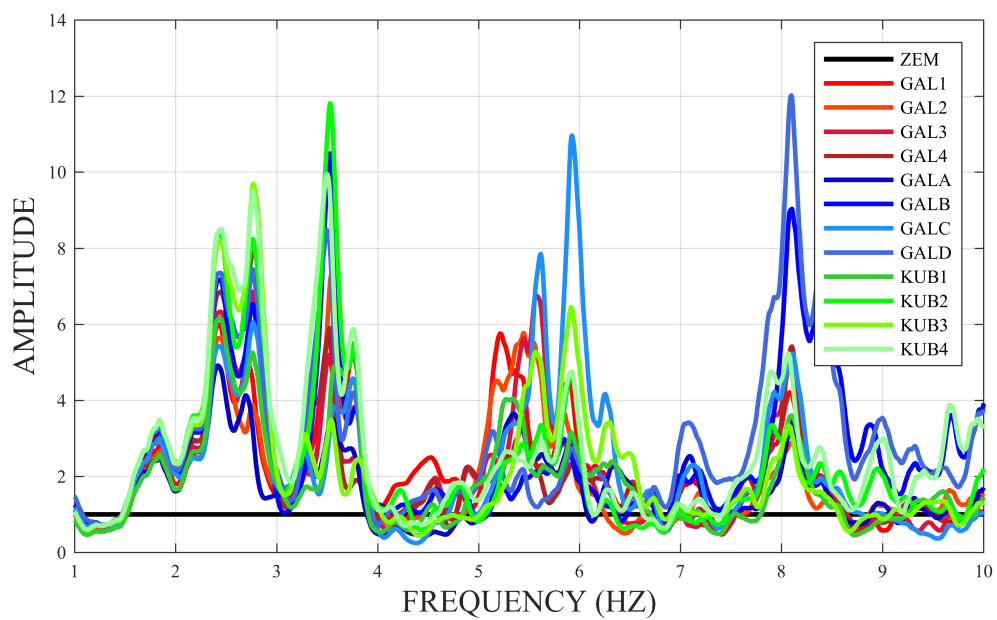


Figure 4.19. Horizontal (Y) top-to-basement Transfer Function of 5.0 Black Sea earthquake

4.2.2. Mode Shapes

Determination of mode shapes is part of system identification. The earthquake data collected from recorders of monitoring system of structures are in time domain, yet the same data can easily be expressed in frequency domain by taking the Fourier transform of the recorded signals. Band-pass filtering is applied to the data around modal frequency to investigate the modal response. The filtered data represent the response at a chosen mode. Mode shapes can be estimated from displacements.

Table 4.2 illustrates the applied band-pass filters to the data around corresponding modal frequencies.

Figure 4.20 shows the particle motions of the mosque during M6.5 Aegean Sea earthquake. It can be easily observed that the mosque is more responsive on the mihrab side especially where GALB, GALC and GALD are located. Modal shapes obtained by filtering around modal frequencies are given in Figures 4.21, 4.22, 4.23, 4.24 and 4.25.

The results from these five earthquake responses evidence that the first frequency in Y direction is relatively smaller than 2.5 Hz, therefore it filtered between 2.3 and 2.5 Hz in general (Figure 4.21). The second mode frequency in X direction may be clearly identified between 2.5 to 2.8 Hz (Figure 4.22). It can be understood from the TF of the records in both direction, the first and the second mode of the mosque is relatively close and it might not be easy to see first two modes in horizontal X and Y transfer function at the same time. For instance, in Figure 4.18 the first mode frequency cannot observe somehow it absorbs. So, when determining the mode shapes we do not interlace the frequencies and apply the filter in a narrow band as much as possible.

Table 4.2. Applied band-pass filter around modal frequencies

	Mode 1	Mode 2	Mode 3	Mode 4	Mode 5
6.5 Aegean Sea	2.3-2.45	2.55-2.80	3.35-3.55	5.1-5.72	7.8-8.2
4.4 Yalova	2.3-2.5	2.60-2.85	3.21-3.60	5.2-5.74	7.8-8.27
4.0 Yalova	2.3-2.5	2.57-2.78	3.35-3.60	5.7-6.1	7.7-8.2
5.6 Romania	2.3-2.5	2.50-2.75	3.32-3.55	5.5-5.62	7.7-8.2
5.0 Black Sea	2.3-2.5	2.5-2.75	3.32-3.55	5.55-5.7	7.8-8.2

Third mode is identified as breathing mode and response to 4.4 Yalova earthquake is displayed in Figure 4.23. The 4th mode is a torsion mode and lastly the 5th mode is determined as squeezing mode which is rather common in historical masonry structures. (Figure 4.24 and Figure 4.25)

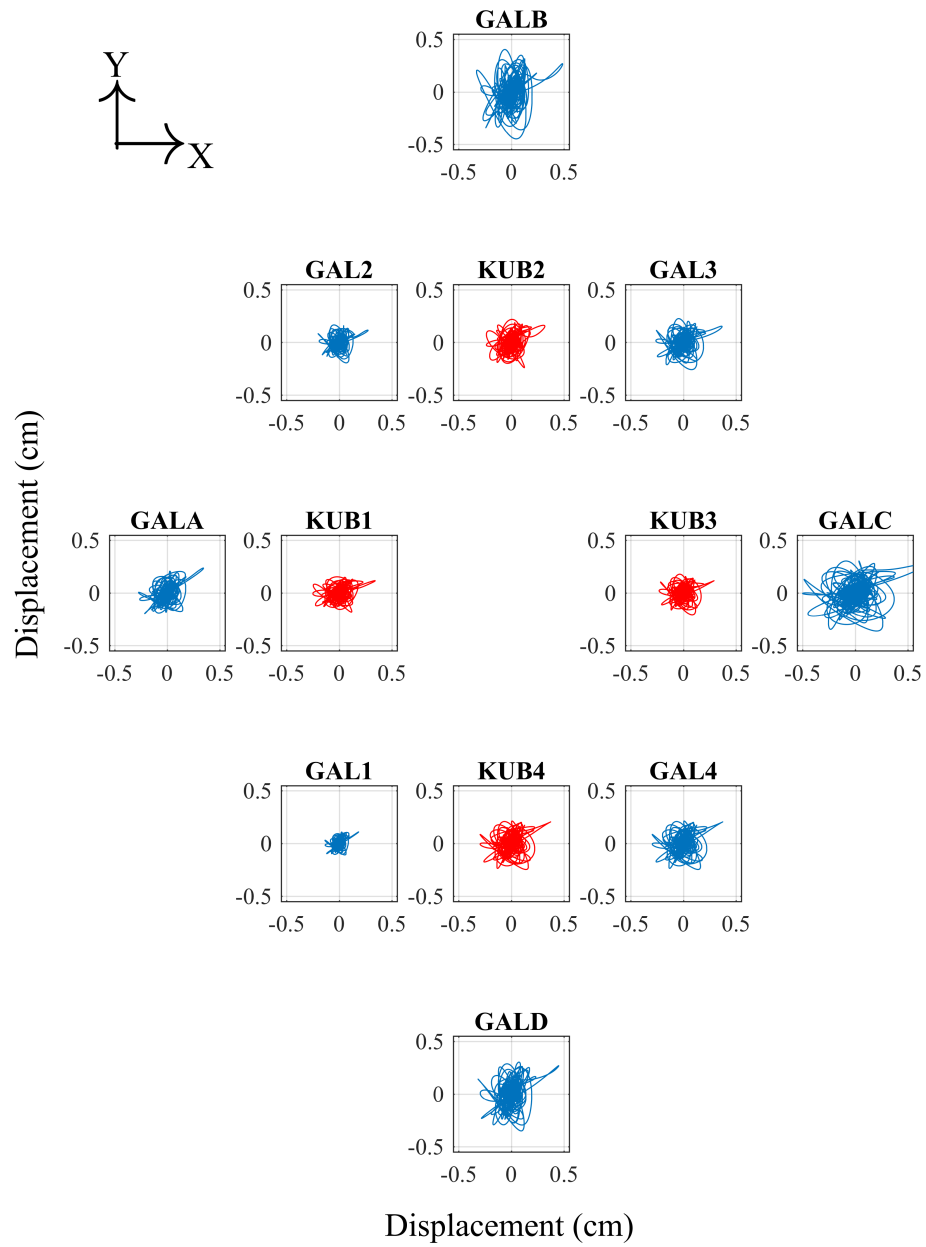


Figure 4.20. Particle motion of the mosque during 6.5 Aegean Sea earthquake

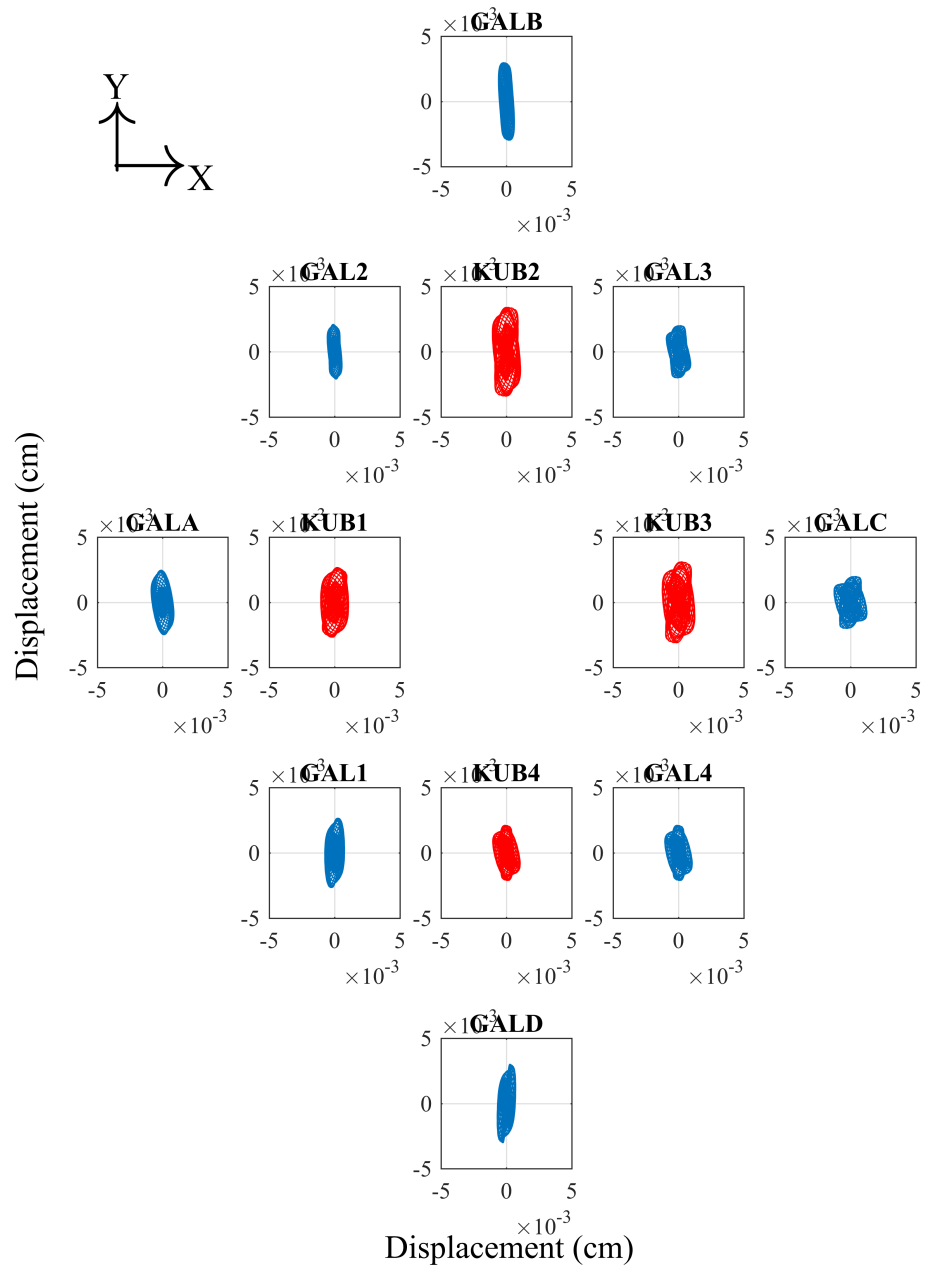


Figure 4.21. Response of the mosque to 5.6 Romania earthquake (Filtered between 2.3 Hz to 2.5 Hz)

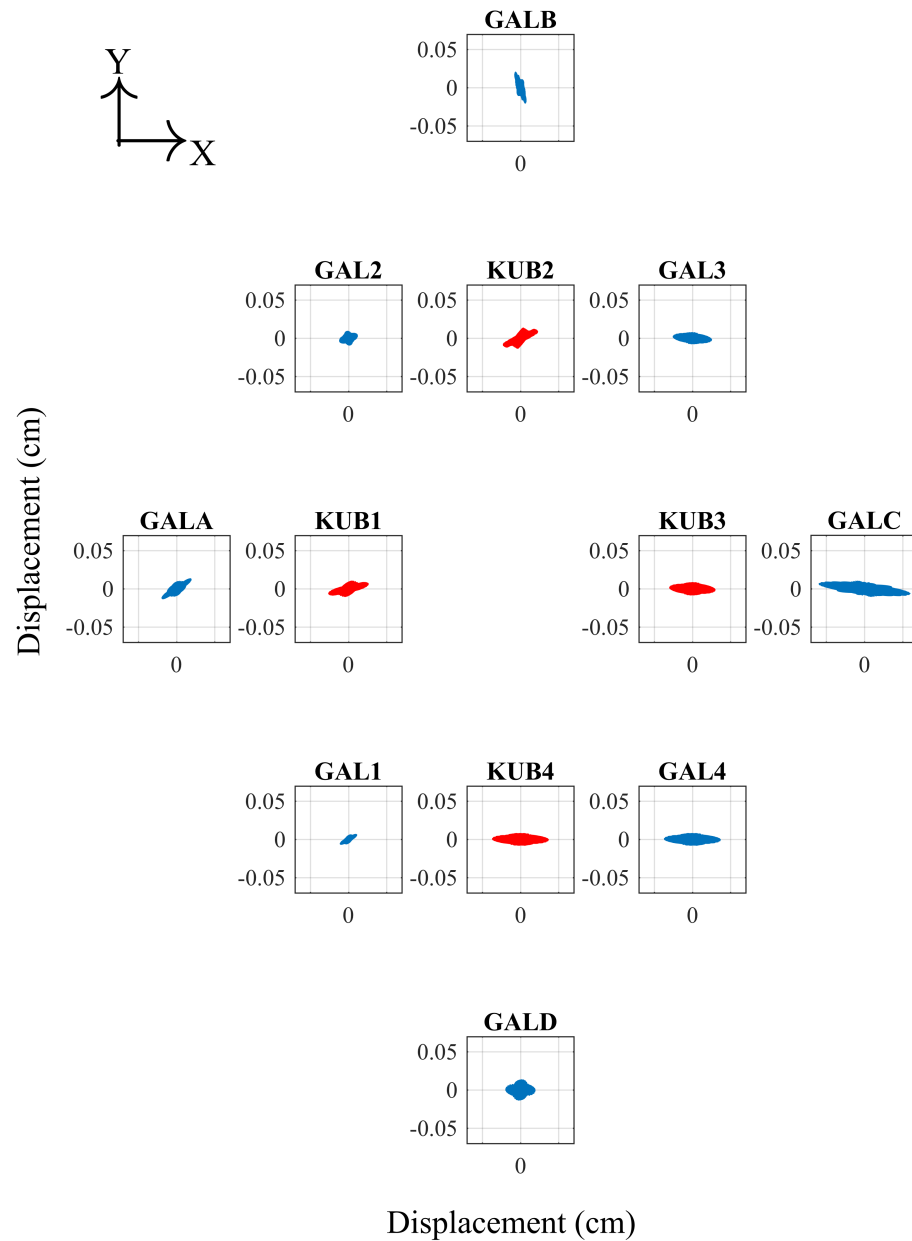


Figure 4.22. Response of the mosque to 6.5 Aegean Sea earthquake (Filtered between 2.55 Hz to 2.80 Hz)

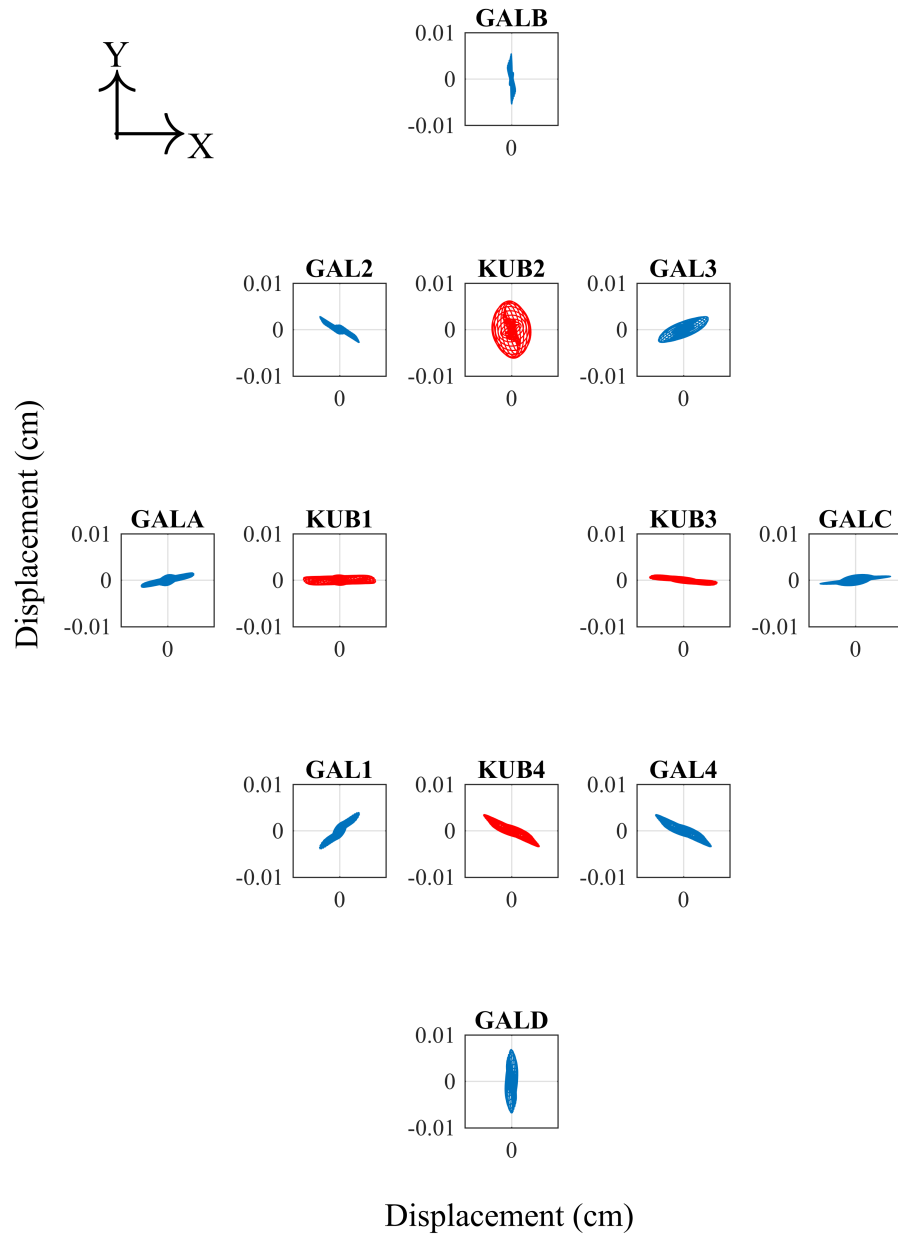


Figure 4.23. Response of the mosque to 4.4 Yalova earthquake (Filtered between 3.21 Hz to 3.60 Hz)

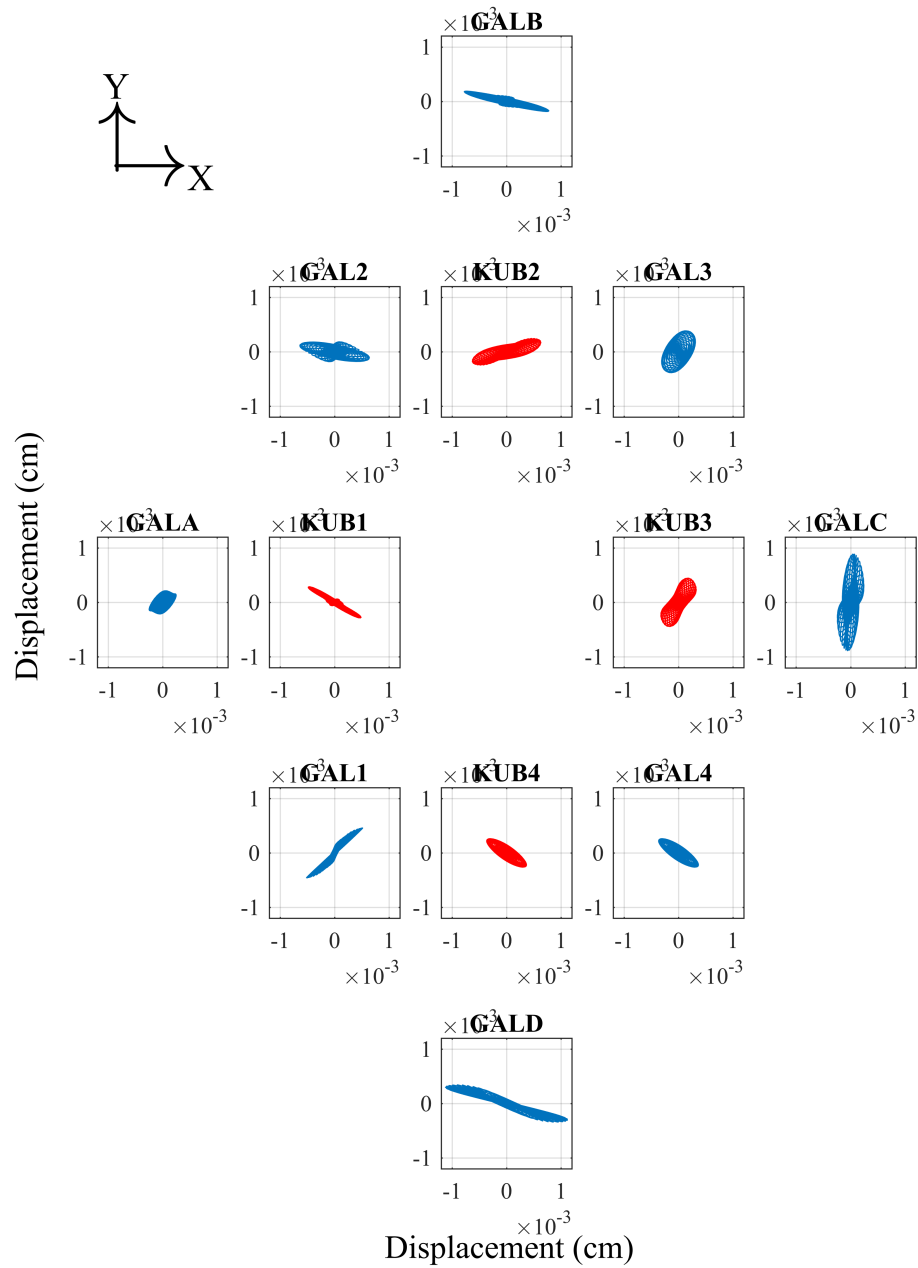


Figure 4.24. Response of the mosque to 4.0 Yalova earthquake (Filtered between 5.7 Hz to 6.1 Hz)

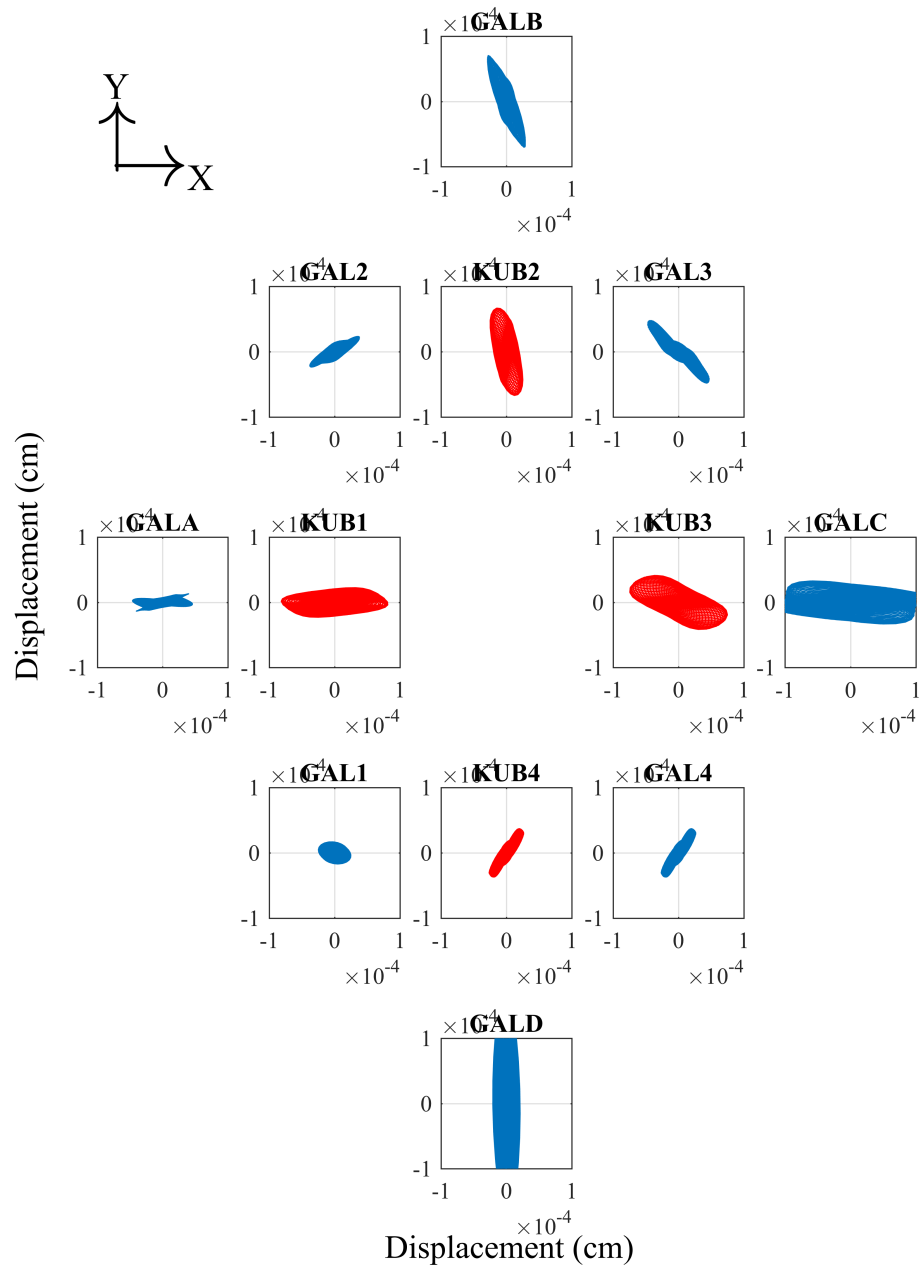
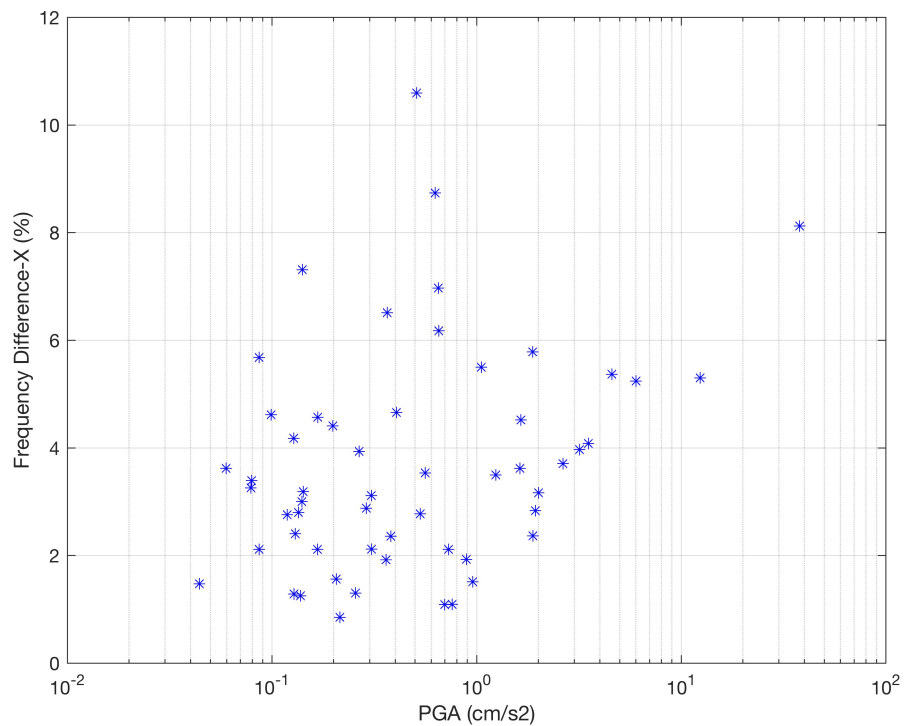


Figure 4.25. Response of the mosque to 4.0 Yalova earthquake (Filtered between 7.7 Hz to 8.2 Hz)

4.2.3. Frequency Change

It is known that the apparent frequency of the structure drops during earthquake and it returns back totally or moderately. We investigate the frequency drop during excitation by comparing the apparent fundamental frequency of record just before the excitation and during excitation. We conclude that the frequency drop is not higher than 15 percent for our dataset.



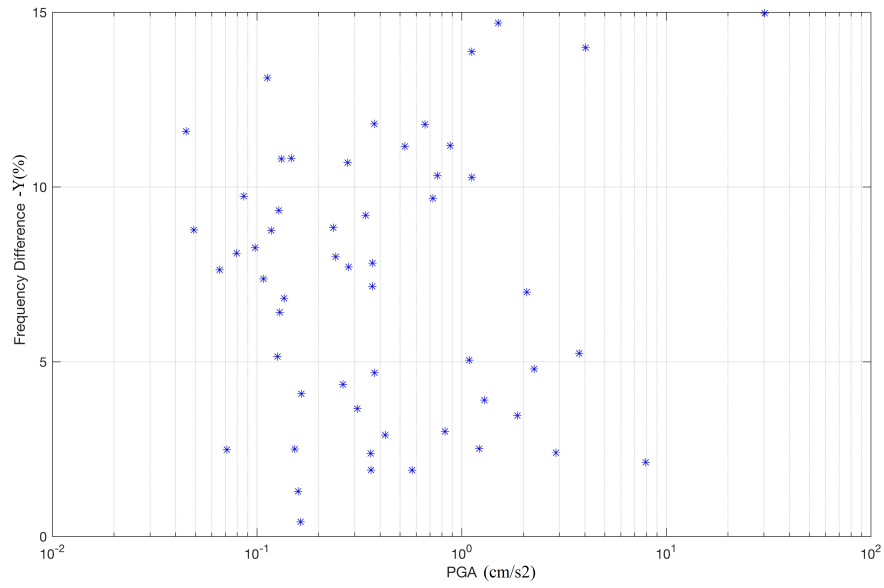


Figure 4.27. Frequency drop in Y direction in percent, horizontal axis is the peak ground acceleration at station ZEM, vertical axis is the frequency change at station KUB3

5. SOIL-STRUCTURE INTERACTION

5.1. Soil-Structure Interaction

Here, we investigate the SSI effects in the mosque by using the recorded seismic events. We follow the systematic attempt suggested by S_{afak} (1988) to identify SSI in the mosque from recorded seismic acceleration data.

SSI can be best determined by comparing the fundamental frequencies of transfer functions and Fourier amplitude spectra of records at the top-stations, because transfer functions are independent of SSI effects and illustrate fixed-base structural behavior.

The five earthquakes shown in Figure 5.1 are utilized in the SSI analysis. Fourier amplitude spectra and transfer functions of three of the earthquakes are displayed in Figures 5.2 , 5.3 5.4, 5.5, 5.6, 5.7, 5.8, 5.9, 5.10, 5.11, 5.12 and 5.13.



Figure 5.1. Earthquakes used in analysis

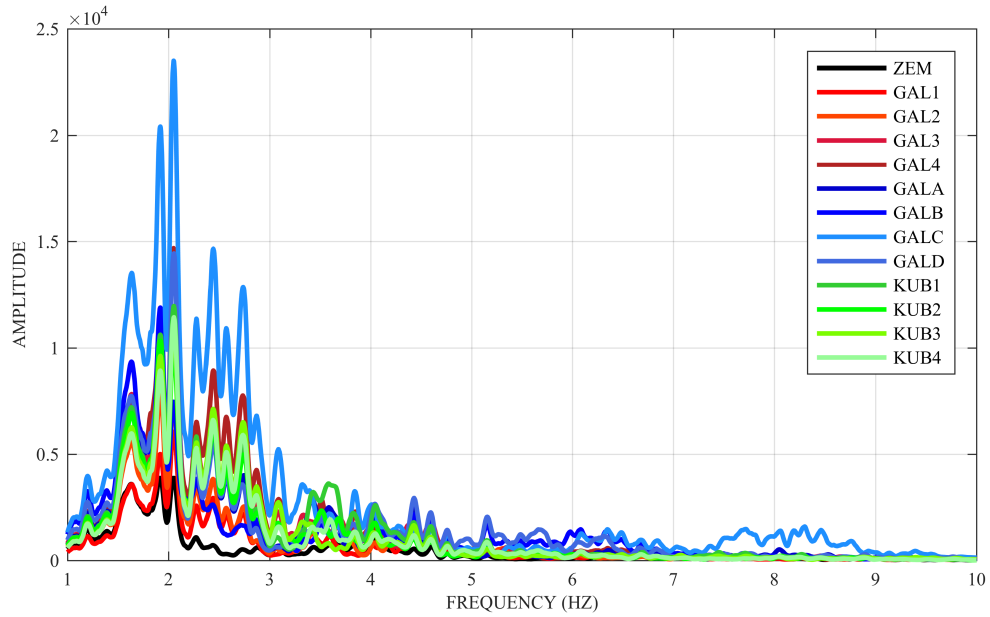


Figure 5.2. Horizontal (X) Fourier Amplitude Spectra of 6.5 Aegean Sea earthquake

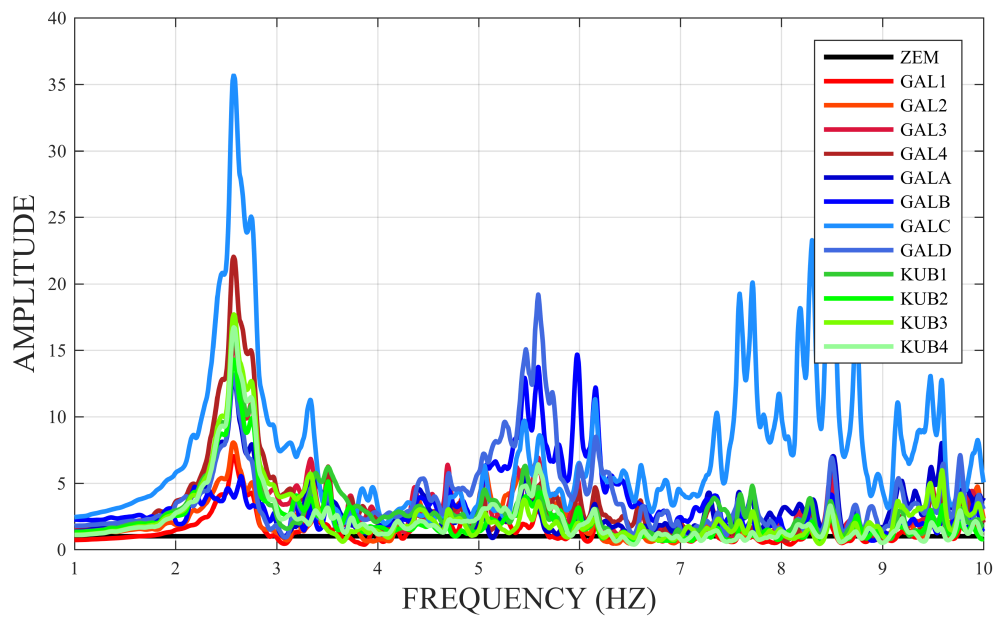


Figure 5.3. Horizontal (X) top-to-basement Transfer Function of 6.5 Aegean Sea earthquake

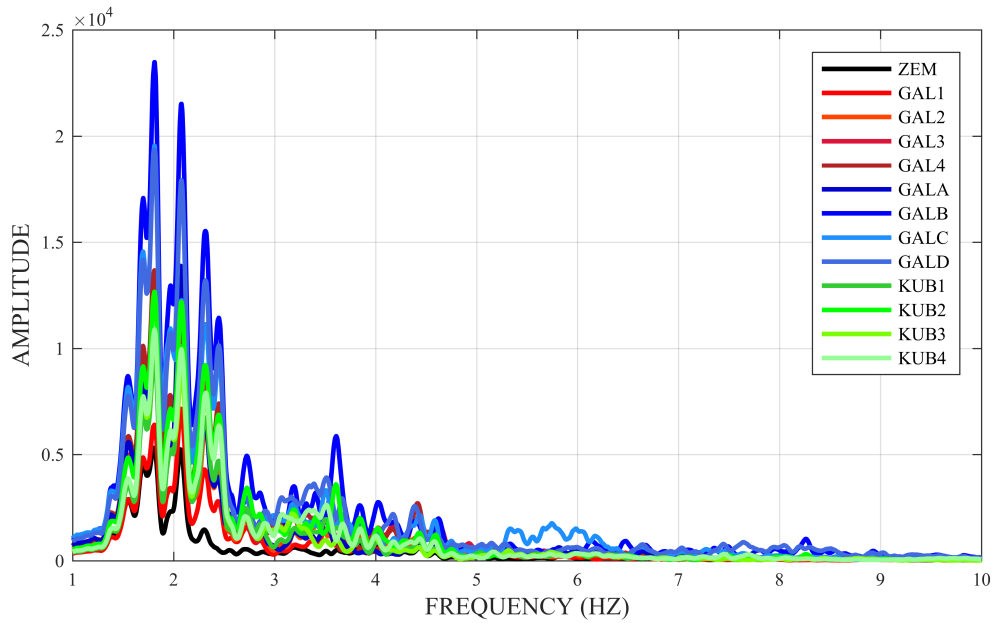


Figure 5.4. Horizontal (Y) Fourier Amplitude Spectra of 6.5 Aegean Sea earthquake

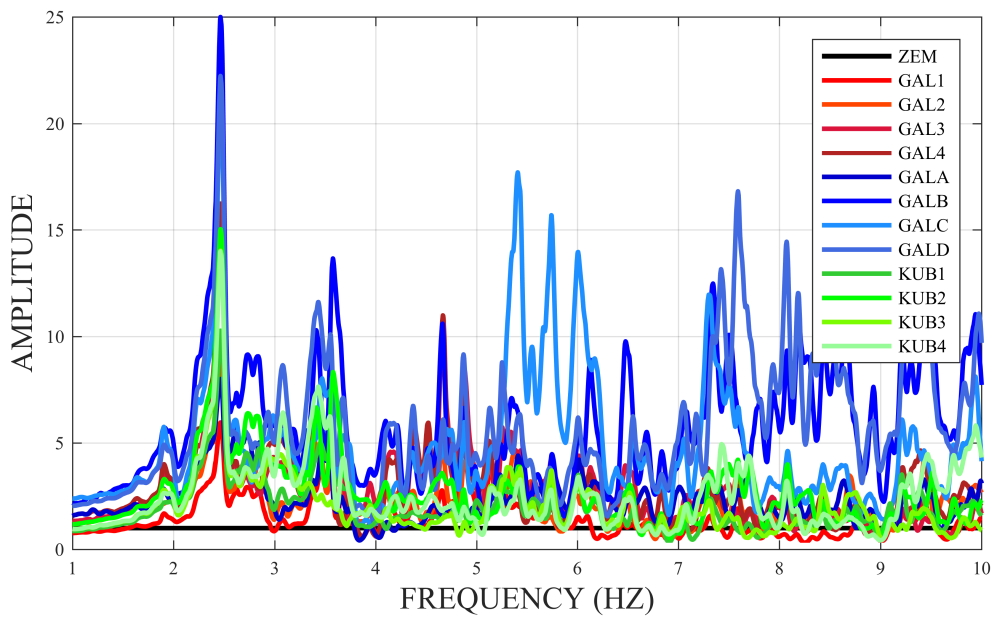


Figure 5.5. Horizontal (Y) top-to-basement Transfer Function of 6.5 Aegean Sea earthquake

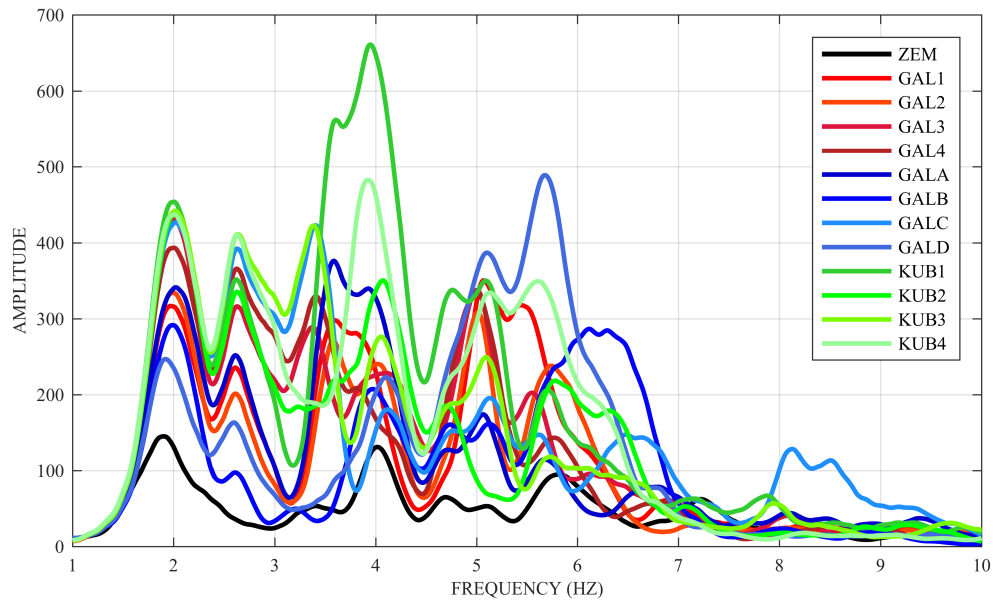


Figure 5.6. Horizontal (X) Fourier Amplitude Spectra of 4.0 Yalova earthquake

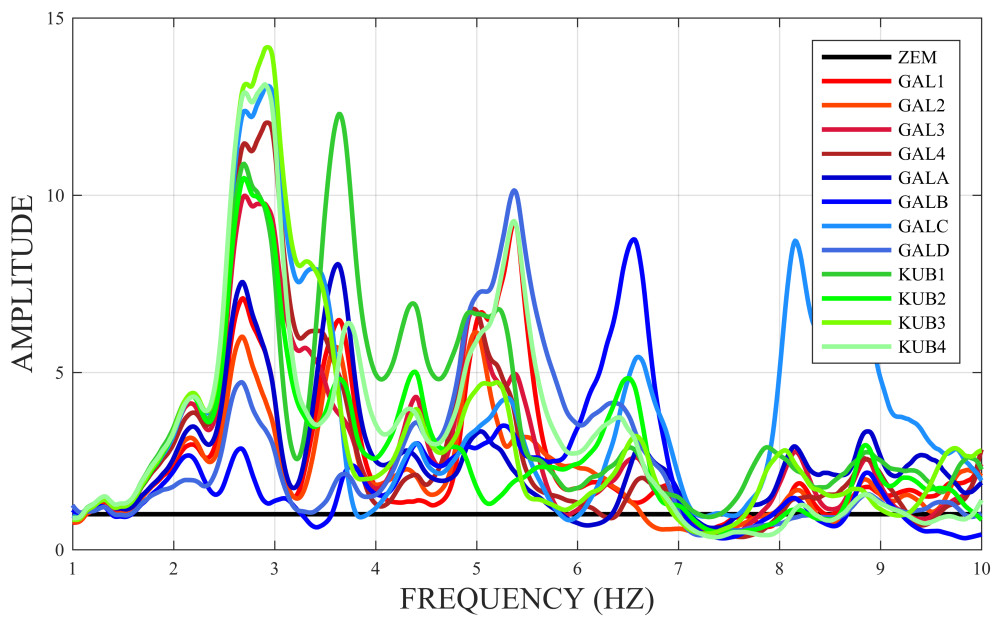


Figure 5.7. Horizontal (X) top-to-basement Transfer Function of 4.0 Yalova earthquake

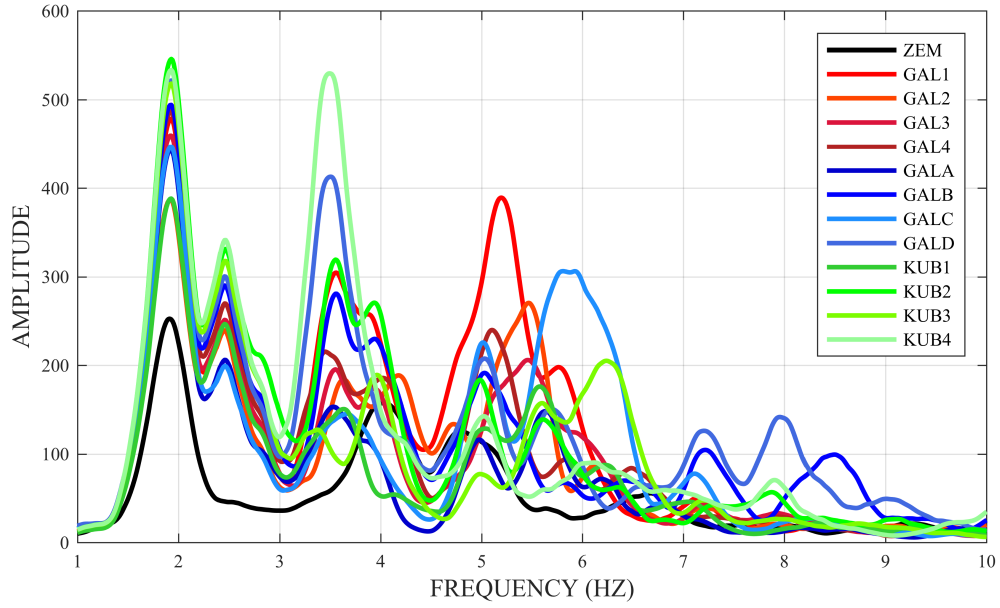


Figure 5.8. Horizontal (Y) Fourier Amplitude Spectra of 4.0 Yalova earthquake

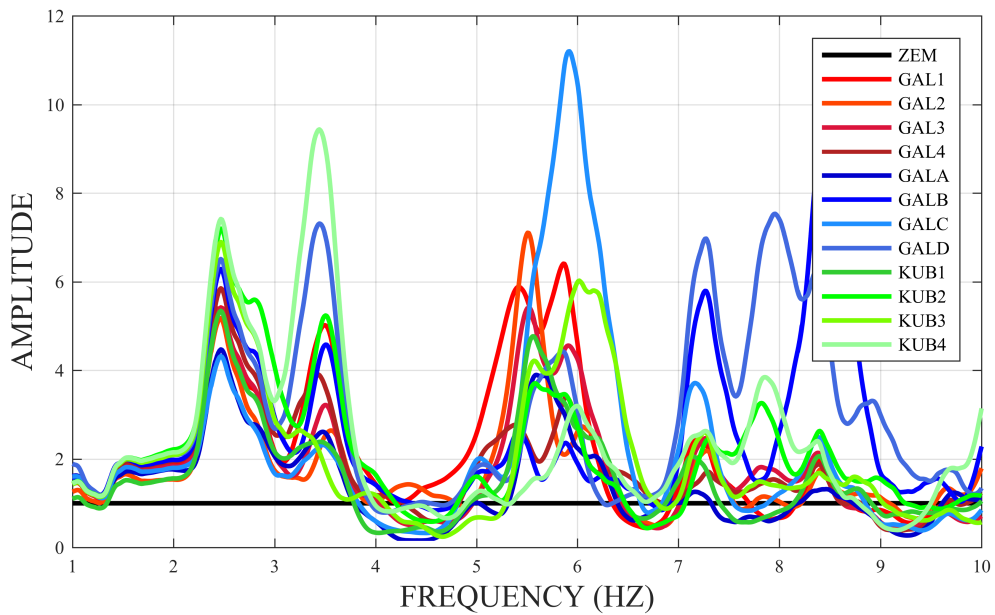


Figure 5.9. Horizontal (Y) top-to-basement Transfer Function of 4.0 Yalova earthquake

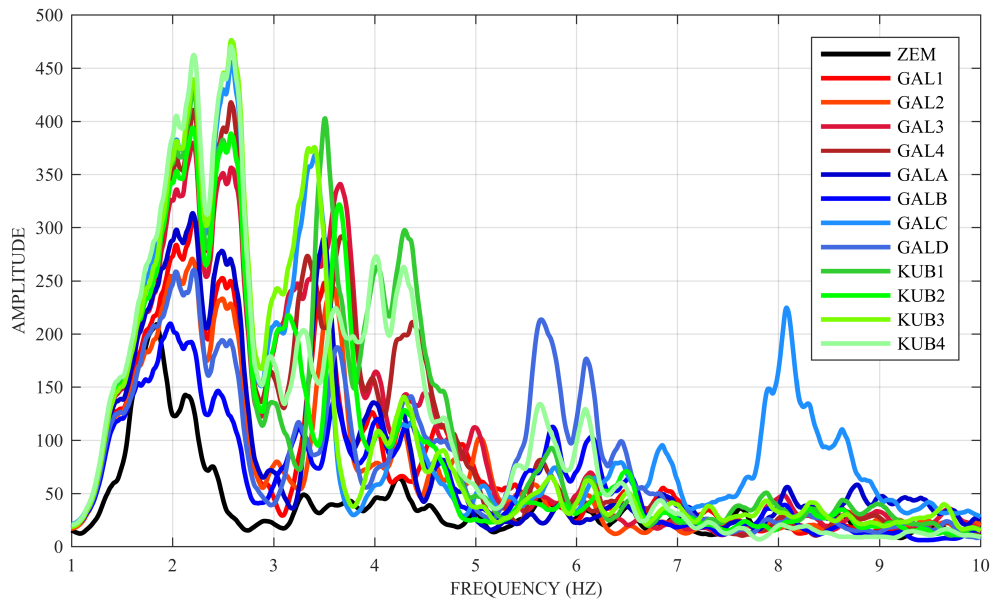


Figure 5.10. Horizontal (X) Fourier Amplitude Spectra of 5.0 Black Sea earthquake

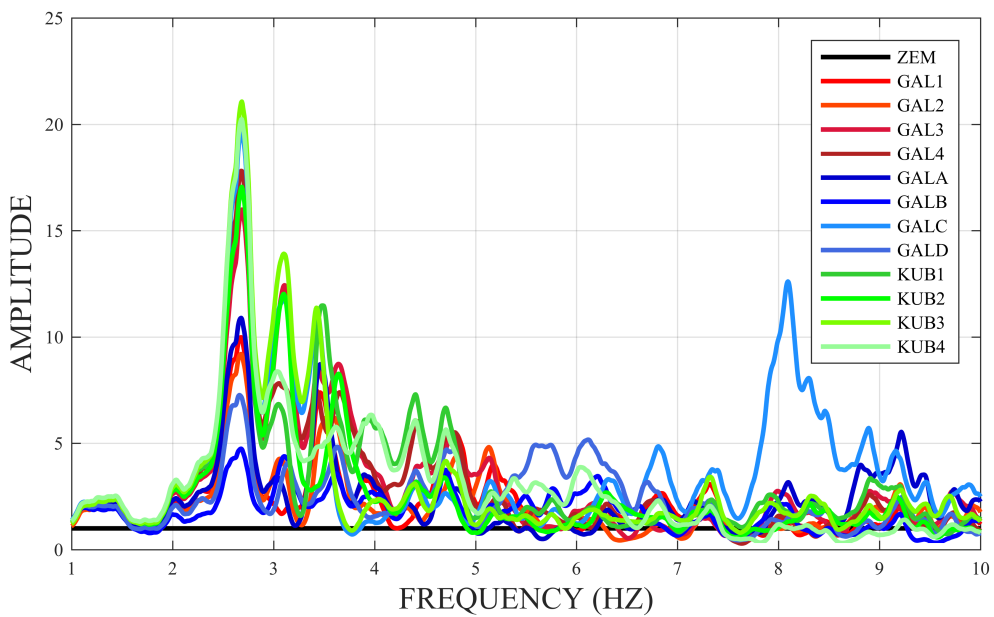


Figure 5.11. Horizontal (X) top-to-basement Transfer Function of 5.0 Black Sea earthquake

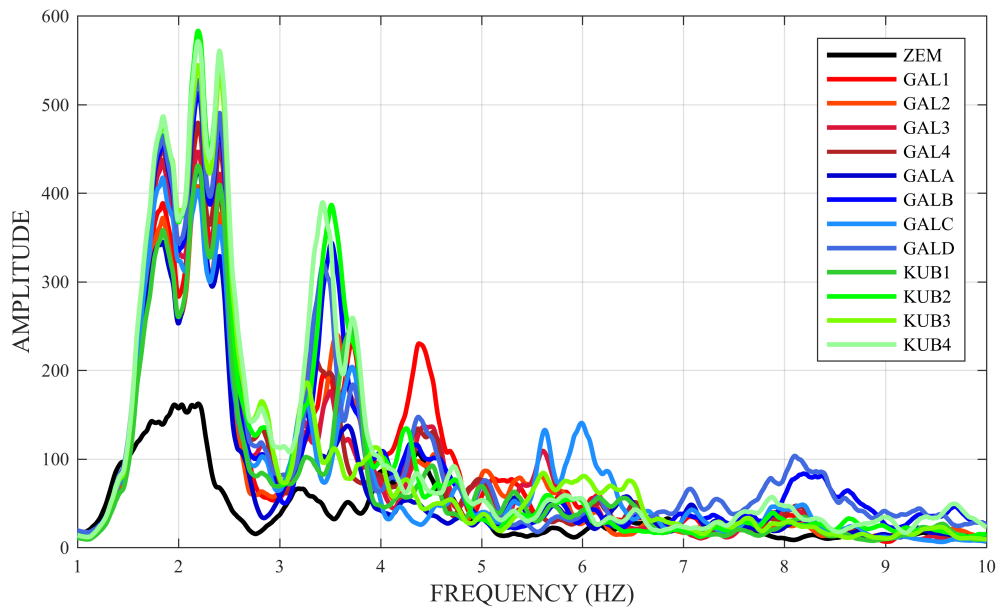


Figure 5.12. Horizontal (Y) Fourier Amplitude Spectra of 5.0 Black Sea earthquake

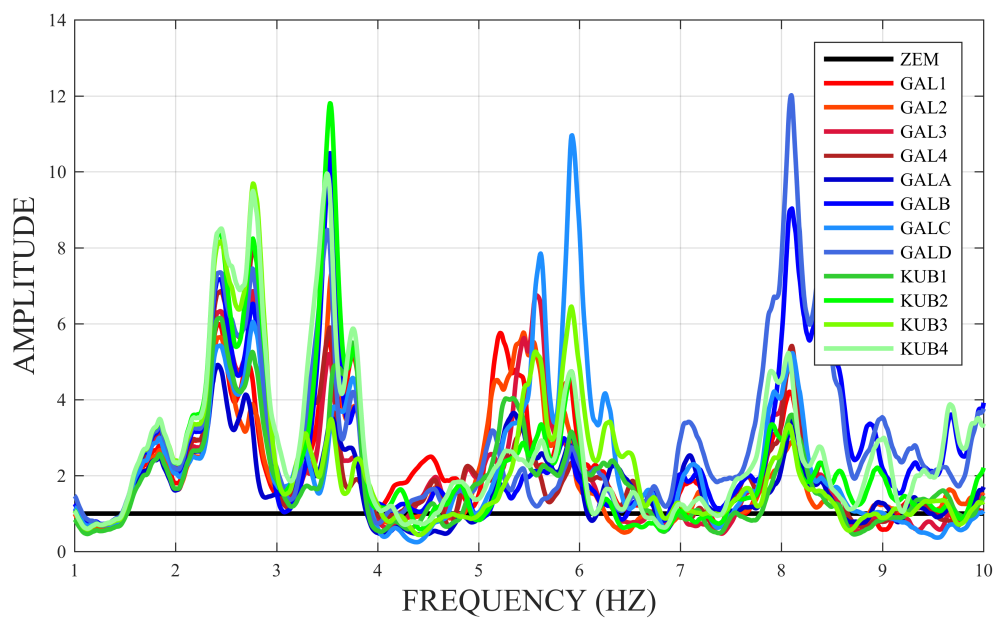


Figure 5.13. Horizontal (Y) top-to-basement Transfer Function of 5.0 Black Sea earthquake

Table 5.1. Fundamental frequencies apparent on horizontal (Y) FAS and TF

	6.5 Aegean Sea	5.6 Romania	4.4 Yalova	4.0 Yalova	5.0 Black Sea
FAS	2.3	2.34	2.34	2.45	2.39
TF	2.47	2.46	2.4	2.48	2.43

Table 5.2. Fundamental frequencies apparent on horizontal (X) FAS and TF

	6.5 Aegean Sea	5.6 Romania	4.4 Yalova	4.0 Yalova	5.0 Black Sea
FAS	2.41	2.67	2.47	2.62	2.58
TF	2.57	2.70	2.75	2.71	2.68

It is well known that the fundamental frequency of a structure with SSI is always smaller than that of the fixed-base structure and of the foundation with no structure present. This SSI effect should be taken into account while identifying the dynamic properties of structures. The numerical values of estimated fundamental horizontal frequencies are presented in Table 5.1 and Table 5.2. It is found that the fundamental frequency evident in FAS is smaller than the fundamental frequency of fixed-based mosque and concluded that mosque is subjected to SSI.

5.2. Soil Effect

Almost all earthquakes considered in this thesis were recorded by the near-by down-hole array, thus allowing further support to investigate the SSI. The fundamental frequency of a structure with SSI is always smaller than that of the fixed-base structure and the data from basement cannot be taken as base excitation.

The underlying soil has been characterized by means of the ground level station in the mosque and the surface station of the down-hole array data. HVSR technique suggests that calculating the ratio between horizontal to vertical Fourier amplitude spectra can identify the fundamental frequency of the foundation soil. Here, we investigate the fundamental soil frequency by recordings at the ground level of the mosque and at the surface station of the down-hole array.

The results of the analyses carried out by Ozaydin et al. (2005) showed that the fundamental frequency at the site of the Fatih mosque is about 2 Hz and the shear wave velocity is 300 m/s. This frequency is also consistent with the fundamental frequency calculated by Kramer's formula (1996) which is 1.97 Hz. Another measurement at the site indicated that the fundamental frequency in NS is 2 Hz and 1.8 Hz in EW direction (Erdik et al., 2004a, b).

In Figure 5.14 and Figure 5.15 the horizontal FAS of ZEM station show peaks at about 1.8 Hz in X direction and Y direction and we know that this frequency is not related to the structure of the mosque itself. On the other hand, the data recorded by surface of down-hole array shows peak around 2 Hz (Figure 5.17, Figure 5.18). In the vertical direction, there is no noticeable peak in FAS of ZEM station (Figure 5.16), yet a peak at 2.27 Hz appears in FAS of surface down-hole array station (Figure 5.19).

From calculated HVSR the fundamental frequency of soil profile appears at 2.1 Hz. (Figure 5.20). Amplitudes drop to 1 that means after this frequency the soil no longer effects the building response.

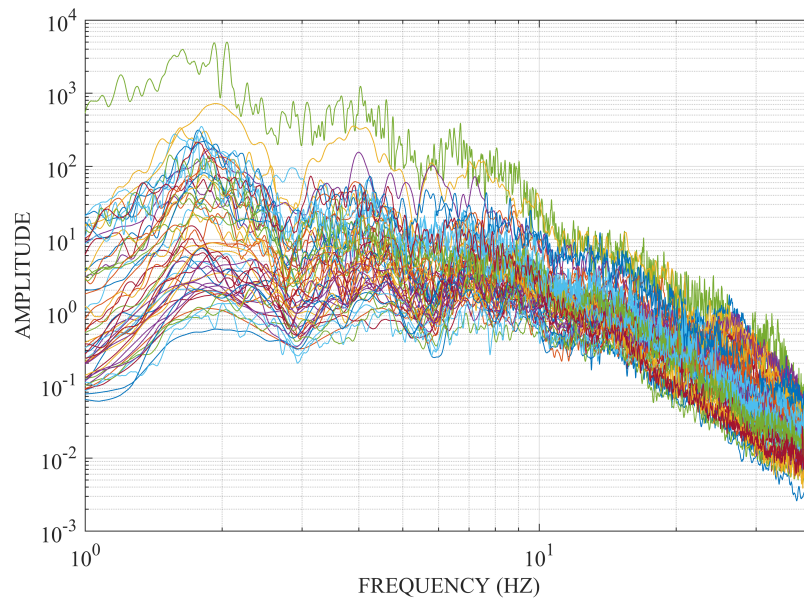


Figure 5.14. Horizontal (X) Fourier amplitude spectra of earthquakes recorded in ZEM station

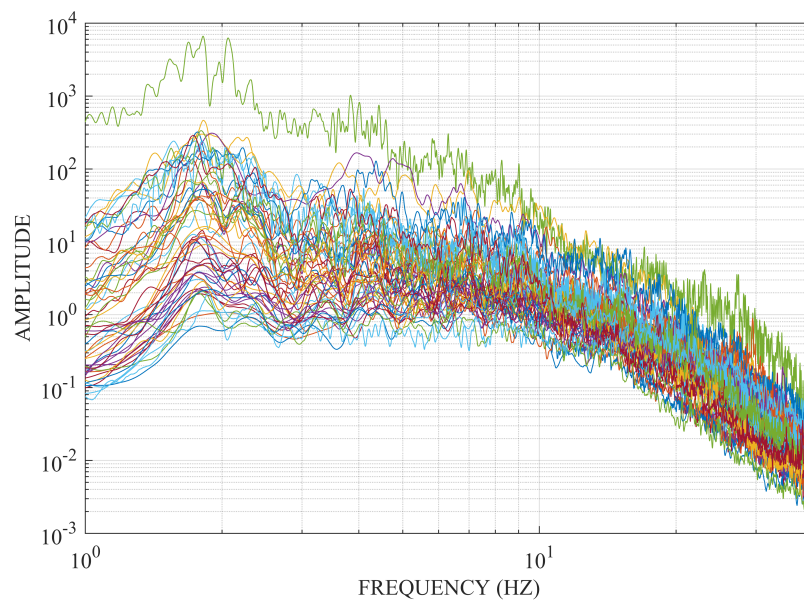


Figure 5.15. Horizontal (Y) Fourier amplitude spectra of earthquakes recorded in ZEM station

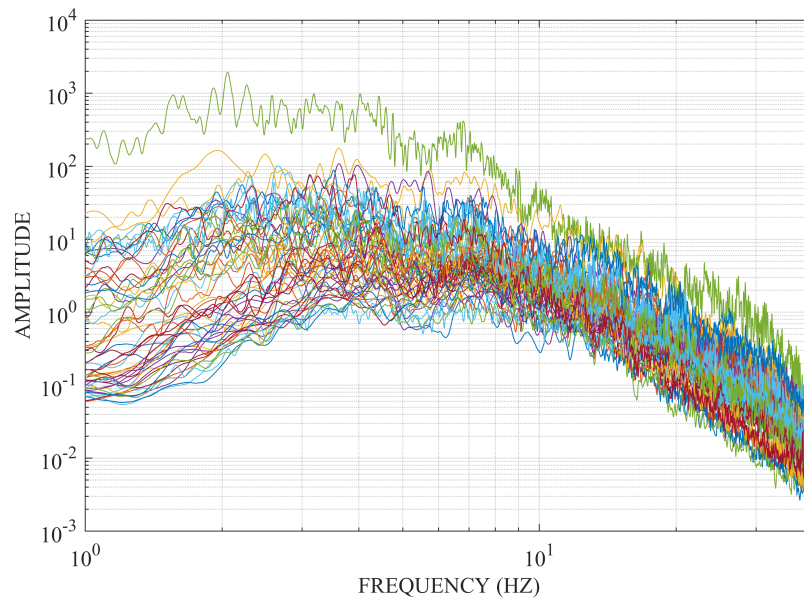


Figure 5.16. Vertical (Z) Fourier amplitude spectra of earthquakes recorded in ZEM station

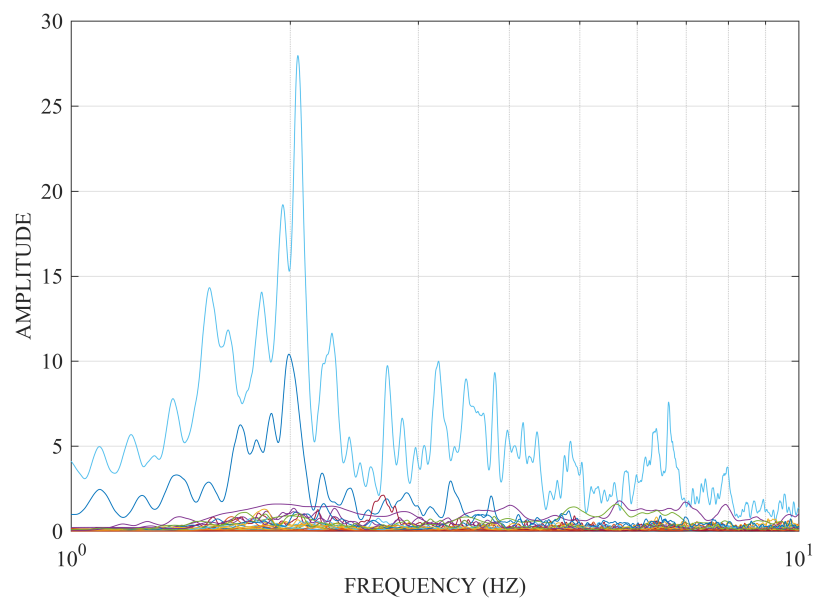


Figure 5.17. Horizontal (X) Fourier amplitude spectra of earthquakes recorded in down-hole

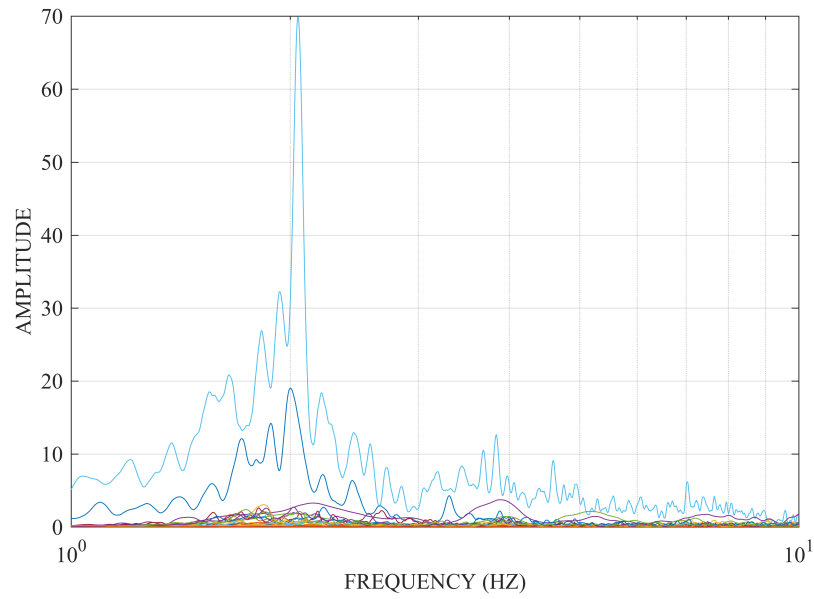


Figure 5.18. Horizontal (Y) Fourier amplitude spectra of earthquakes recorded in down-hole

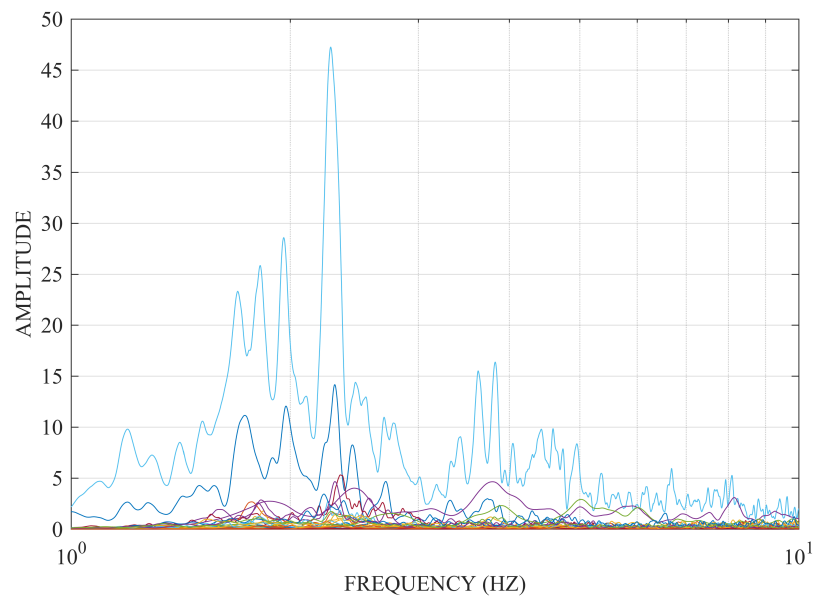


Figure 5.19. Vertical (Z) Fourier amplitude spectra of earthquakes recorded in down-hole

Records obtained from the strong motion network shows that the frequencies below 2.1 Hz are generated by the underlying sediments and not related to the structural system. This can be best observed in the difference in frequency content of TF and FAS of the mosque. In transfer functions we cannot see frequencies below 2 Hz which are apparent in FAS of records.

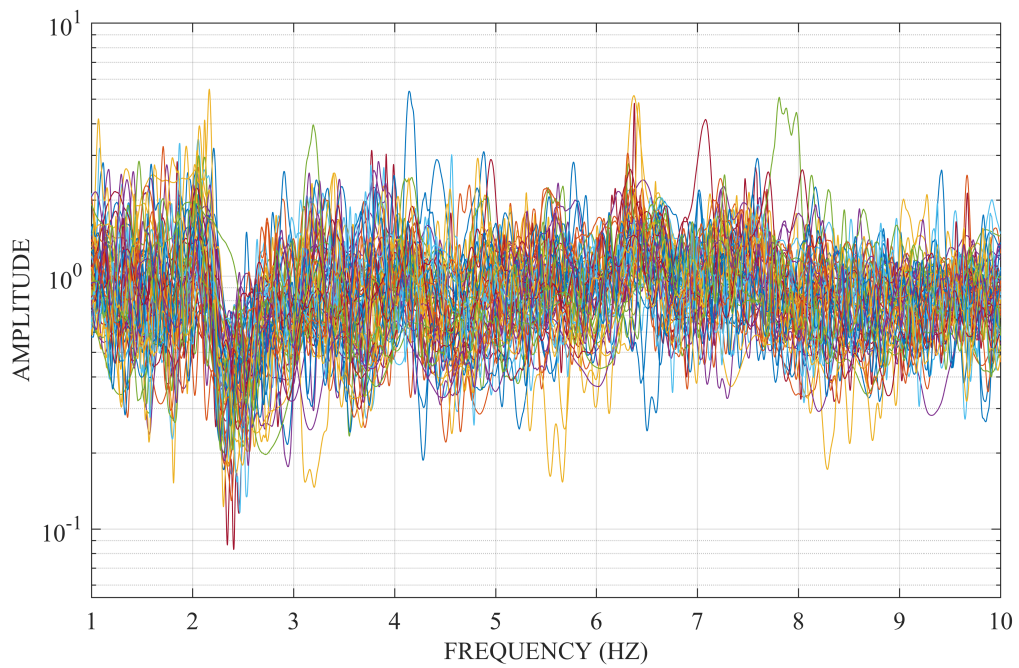


Figure 5.20. Horizontal to vertical spectral ratio of Fas of down-hole surface array of Fatih

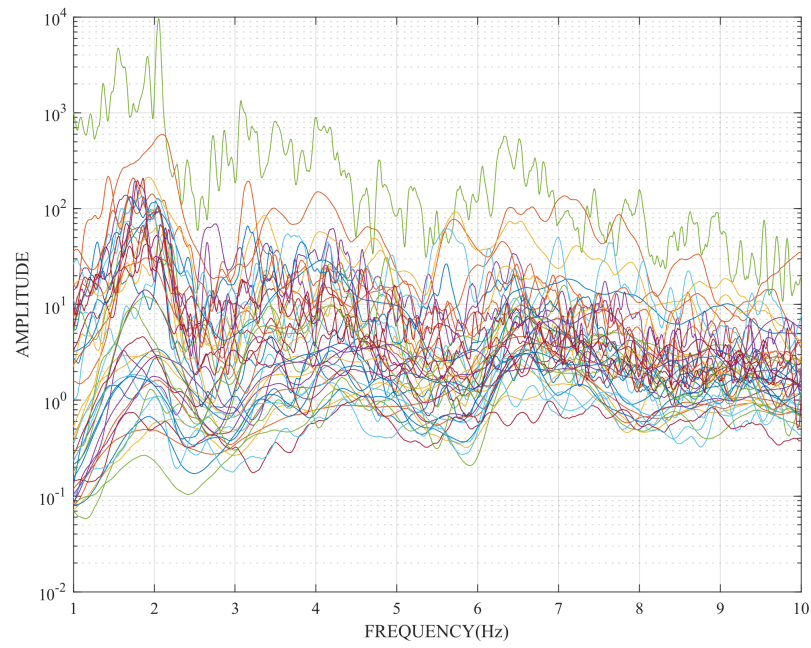


Figure 5.21. Horizontal to vertical spectral ratio of Fas of ZEM station of Fatih

6. ROCKING

Rocking is a specific response type also known as ‘rigid body motion’. There are a couple of techniques to identify rocking response of structures. They depend on the investigation of records representative of the geometry of rocking and are based on vertical movement of foundation and horizontal movement of top floors. The most common way to identify rocking mode is first taking the differences of two vertical records from the foundation and applying band-pass filter to the data around rocking frequency. The rocking frequency can also be identified by finding a similar frequency range with identical peaks in the Fourier amplitude Spectra of the vertical records from foundation and of horizontal records from upper stories. However, in Fatih Mosque’s SHM system there is only one accelerometer in the ground level. Therefore we use the second approach by studying ZEM station’s vertical component and two- horizontal components of GAL1, GAL2, GAL3 and GAL4 stations. The reason why we select GAL1, GAL2, GAL3 and GAL4 stations and not dome level stations, is that these stations are located on the main pillars and therefore geometrically favorable.

The simplest way to investigate the existence of rocking vibrations in a building is to find a common frequency between foundation and top floors. In our case the mosque is subjected to SSI, so first looking at the Fourier amplitude spectra to find a common frequency and then to look for the same frequency in foundation-to-top-floors horizontal transfer functions and vertical direction Fourier amplitude spectra at foundation/ground level should suffice to investigate rocking vibrations, because during rocking vibrations the structure is assumed to rotate like a rigid block and transfer functions are best representations of fixed-base structural response in frequency domain.

In Figure 6.1 Fourier amplitude spectra of ZEM, GAL1, GAL2, GAL3 and GAL4 stations in two horizontal directions for the M6.5 Aegean Sea earthquake are given. At first glance, it seems there are common peaks in the frequency range of 1.5 Hz to 3 Hz and it is worthwhile to investigate them separately.

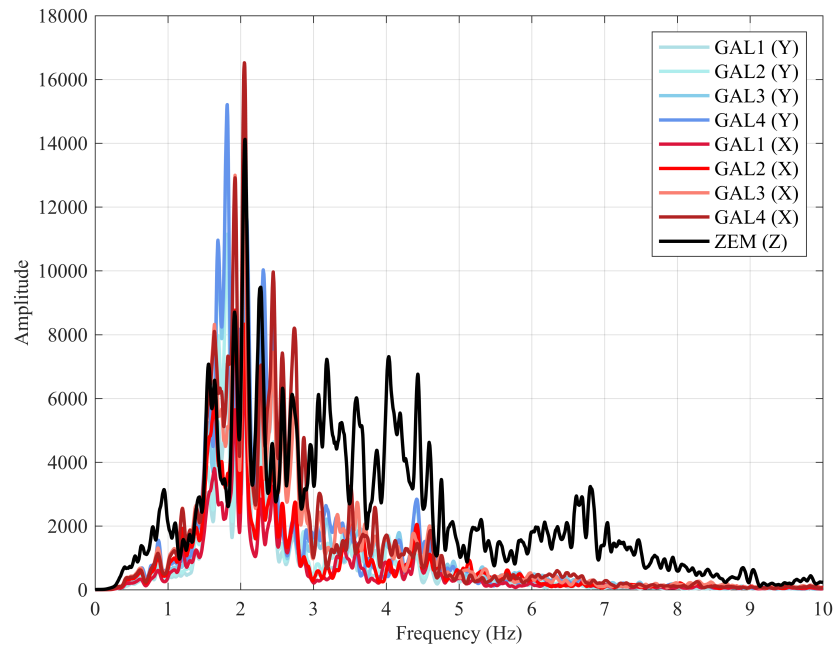


Figure 6.1. Fourier amplitude spectrum of vertical ZEM and horizontal components (X and Y) of GAL1, GAL2, GAL3, GAL4 stations

In X direction, the common peaks in horizontal Fourier amplitude spectra of GAL stations and vertical Fourier amplitude spectrum of ZEM (Figure 6.2) station can be estimated as 1.65, 1.92, 2.06, 2.27, 2.43, 2.57 and 2.7 Hz. Afterwards, one of these frequencies should be observed in foundation-to-top-floor transfer functions to call it ‘rocking vibration frequency.’ Figure 6.3 represents the foundation-to-top-floor transfer functions in X direction and vertical Fourier amplitude spectrum of ZEM station. Only two frequencies remain which are around 2.43 Hz and 2.57 Hz, yet we know former studies (modal analysis) that these frequencies belong to the structure and were interpreted as first modal frequency in Y direction and second modal frequency in X direction.

The same process can be done for investigation of rocking vibrations in Y direction. Looking at Figure 6.4 which illustrates horizontal Fourier amplitude spectra of GAL stations and vertical Fourier amplitude spectrum of ZEM station, the common peaks determined as as 1.56, 2.06, 2.27 and 2.45 Hz. Nevertheless only 2.45 Hz remains as the common frequency in the foundation-to-top-floor transfer functions in X direction and Fourier amplitude spectrum of ZEM station (Figure 6.5), this vibration frequency belongs to first modal vibration of structure dominant in Y direction.

Depending on all studies we conclude that the mosque is not subjected to rocking vibrations neither in X nor Y in direction.

Rocking vibrations are the rigid body vibrations of a structure with respect to its foundation and most seen in tall buildings. Here, the existence of rigid body vibrations were investigated in a historical mosque.

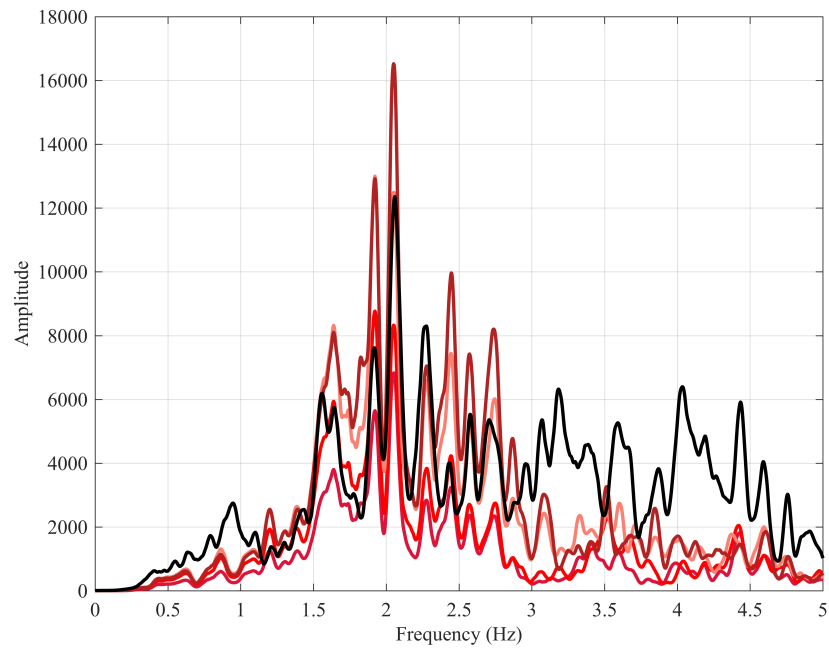


Figure 6.2. FAS of 6.5 Aegean Sea Earthquake (X direction)

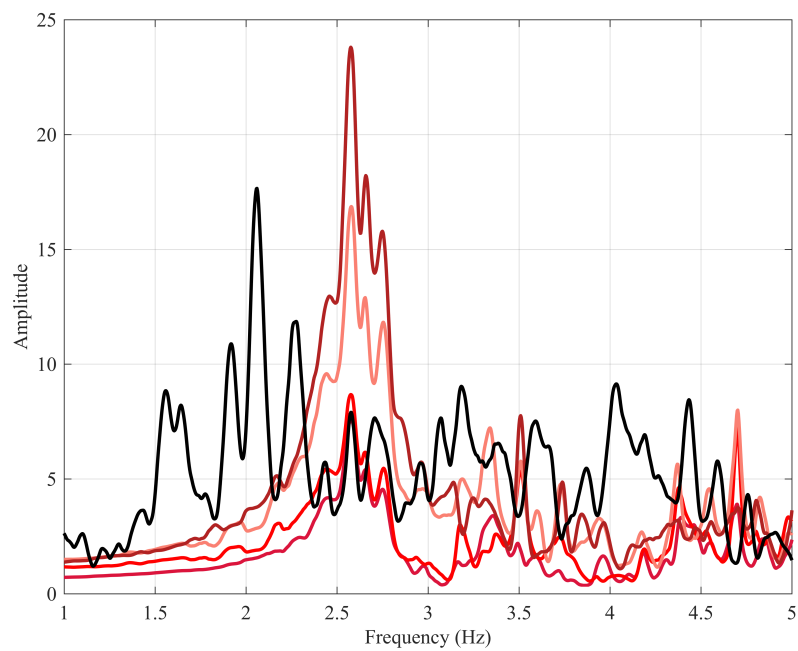


Figure 6.3. TF of 6.5 Aegean Sea Earthquake (X direction)

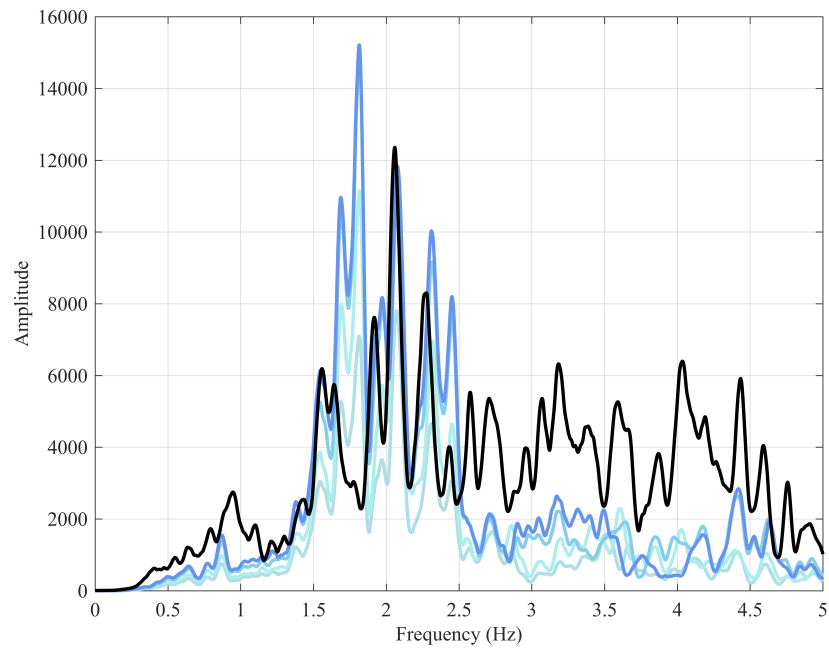


Figure 6.4. FAS of 6.5 Aegean Sea Earthquake (Y direction)

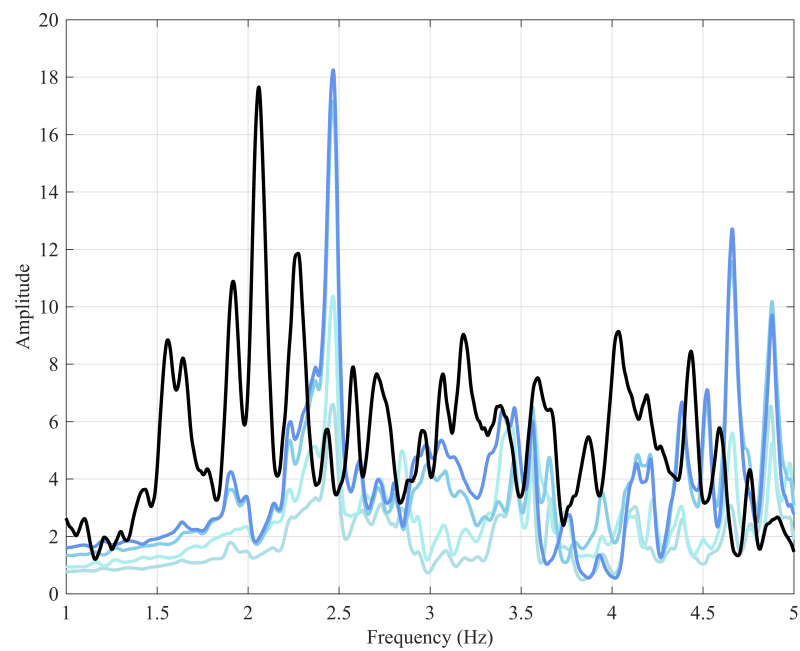


Figure 6.5. TF of 6.5 Aegean Sea Earthquake (Y direction)

7. WAVE TRAVELS

In a situation, where the system response changes from linear to nonlinear, time histories alone could be sufficient to identify damage. When structures behave in nonlinear range the dynamic properties change and consequently modal parameters change as well. Generally, nonlinear behavior causes decrease in stiffness and consequently an increase in natural period is observed. However, modal parameters are not sensitive to local or small damages. In that case, wave propagation approach is a more convenient method to identify local damages.

In monitored structures, the damage can be investigated in terms of the difference of wave travel times between locations of accelerometers. Sampling rate should be high enough to catch the travel time. In Fatih Mosque, the shear wave velocity is estimated to be between 350 m/s and 400 m/s. The height between the base and gallery level is about 17.5 m, so the difference in wave arrivals is expected to be 0.045 seconds. The 200 Hz sampling rate is enough to detect variations in wave velocities due to local damages.

First of all, to apply the wave propagation approach the data in all channels and instruments should be synchronized and the sampling rate should be high enough to catch the travel times between two locations in the building. However, in Fatih's SHM system the ground level station had timing problems such that the data were not finely synchronized with upper levels. Therefore damage detection by wave propagation approach could not be attempted. It is significant to note that interesting results could have been derived with fully synchronized data and also additional instruments.

8. CONCLUSION

The structural response to external forces is a crucial issue for conservation of historical heritage buildings and also for modern structural engineering applications. In this study an historical mosque located in Fatih district of Istanbul, which known as the Conqueror's mosque, was selected with the aim of investigating its dynamic response characteristics by means of earthquake recordings provided by the monitoring system.

First of all, by analyzing the data in time domain it is found that the mosque is more responsive through on its mihrab side (south-east) of the mosque and there is a moderate correlation between the magnitude of the excitation and the response of the mosque. Additional measurements and studies are recommended on the site to investigate the underlying reasons for the relatively large response of the mihrab side of the the mosque. The first modal frequency is determined as 2.45 Hz dominant in Y direction while the second modal frequency as 2.74 Hz dominant in X direction. Up to 15% decrease can be expected in the modal frequencies of the Fatih mosque during earthquakes.

Analysis performed to investigate the presence of soil-structure interaction and rigid body vibrations yielded that the response of the Fatih Mosque is affected by soil structure interaction, due to which a decrease in apparent fundamental frequency is observed. The mosque is found not to experience any rigid body vibrations.

A damage detection by investigating the delays between wave arrival times between different stations is attempted. However, it was found that the monitoring system is not finely synchronized due to some technical problems. The stations should be fully synchronized to be able to carry out the wave propagation analysis for estimation of wave travel times.

REFERENCES

1. Udwadia, F. and M. Trifunac, “Time and amplitude dependent response of structures”, *Earthquake Engineering & Structural Dynamics*, Vol. 2, No. 4, pp. 359–378, 1973.
2. Todorovska, M., M. Trifunac and T.-y. Hao, “Variations of apparent building frequencies-lessons from full-scale earthquake observations”, *Proc. First European Conf. on Earthquake Engineering and Seismology*, pp. 3–8, 2006.
3. Todorovska, M. I. and Y. Al Rjoub, “Effects of rainfall on soil–structure system frequency: examples based on poroelasticity and a comparison with full-scale measurements”, *Soil Dynamics and Earthquake Engineering*, Vol. 26, No. 6, pp. 708–717, 2006.
4. Şafak, E., “Detection and identification of soil-structure interaction in buildings from vibration recordings”, *Journal of Structural Engineering*, Vol. 121, No. 5, pp. 899–906, 1995.
5. Şafak, E., “New approach to analyzing soil-building systems”, *Soil Dynamics and Earthquake Engineering*, Vol. 17, No. 7, pp. 509–517, 1998.
6. Uzgider, E. and M. Aydogan, “Simple and efficient method for the dynamic response of 2D frames subject to ground motions”, *Proc. 8th European Conf. on Earthquake Engineering*, pp. 7–12, 1986.
7. Freely, J., *A history of Ottoman architecture*, WIT Press, 2011.
8. Mazlum, D., *Osmanlı Arşiv Belgeleri Işığında 22 Mayıs 1766 İstanbul Depremi ve Ardından Gerçekleştirilen Yapı Onarımları*, Ph.D. Thesis, Fen Bilimleri Enstitüsü, 2015.

9. Köse, F., “Arşiv Belgelerine Göre Fatih Camiinin İnşaası ve Onarımları” , , 2013.
10. Aga-Oglu, M., “The Fatih Mosque at Constantinople”, *The Art Bulletin*, Vol. 12, No. 2, pp. 179–195, 1930.
11. Ceylan, O. and T. K. Ocakcan, “Fatih Camii 2007-2012 RestoRasyonu uygulamaları”, , 2013.
12. Çılı, F. and H. Yıldız, “Fatih Camii ve I. Mahmut Kütüphanesi Güçlendirme Çalışmaları” , , 2013.
13. Berilgen, M., “Evaluation of local site effects on earthquake damages of Fatih Mosque”, *Engineering geology*, Vol. 91, No. 2, pp. 240–253, 2007.
14. D’Ambrisi, A., V. Mariani and M. Mezzi, “Seismic assessment of a historical masonry tower with nonlinear static and dynamic analyses tuned on ambient vibration tests”, *Engineering Structures*, Vol. 36, pp. 210–219, 2012.
15. Chaudhary, M., M. Abe and Y. Fujino, “Identification of soil–structure interaction effect in base-isolated bridges from earthquake records”, *Soil Dynamics and Earthquake Engineering*, Vol. 21, No. 8, pp. 713–725, 2001.
16. Todorovska, M. I. and M. D. Trifunac, “Earthquake damage detection in the Imperial County Services Building I: The data and time–frequency analysis”, *Soil Dynamics and Earthquake Engineering*, Vol. 27, No. 6, pp. 564–576, 2007.
17. Todorovska, M. I. and M. D. Trifunac, “Earthquake damage detection in the Imperial County Services Building III: analysis of wave travel times via impulse response functions”, *Soil Dynamics and Earthquake Engineering*, Vol. 28, No. 5, pp. 387–404, 2008.
18. Bongiovanni, G., M. Celebi and E. Safak, “Seismic rocking response of a triangular building founded on sand”, *Earthquake spectra*, Vol. 3, No. 4, pp. 793–809, 1987.

19. Doebling, S. W., C. R. Farrar, M. B. Prime *et al.*, “A summary review of vibration-based damage identification methods”, *Shock and vibration digest*, Vol. 30, No. 2, pp. 91–105, 1998.
20. Yetkin, S. K., “The Evolution of Architectural Form in Turkish Mosques (1300-1700)”, *Studia Islamica*, , No. 11, pp. 73–91, 1959.
21. Ivanovic, S., M. Trifunac and M. Todorovska, “On identification of damage in structures via wave travel times”, *Strong Motion Instrumentation for Civil Engineering Structures*, pp. 447–467, 2001.
22. Ambraseys, N. N. and C. Finkel, “The Marmara sea earthquake of 1509”, *Terra Nova*, Vol. 2, No. 2, pp. 167–174, 1990.
23. Todorovska, M. I., “Separation of the Effects of Soil-Structure Interaction in Frequency Estimation of Buildings From Earthquake Records”, *Coupled Site and Soil-Structure Interaction Effects with Application to Seismic Risk Mitigation*, pp. 169–178, 2009.
24. Safak, E., E. Cakti and Y. Kaya, “Seismic wave velocities in historical structures: a new parameter for identification and damage detection”, *Proceedings of (IOMAC 2009) the 3rd international modal analysis conference, Ancona, Italy*, pp. 4–6, 2009.
25. Hayashi, Y. and I. Takahashi, “Soil-structure interaction effects on building response in recent earthquakes”, *Third UJNR Workshop on Soil-Structure Interaction Vallombrosa Center, Menlo Park, California*, 2004.
26. Kunter, H. B. and A. S. Ülgen, *Fatih camii ve Bizans sarnıcı*, Cumhuriyet Matbaası, 1939.